

ANNUAL REPORT





Nuclear Science User Facilities 995 MK Simpson Blvd. Idaho Falls, ID 83401-3553 nsuf.inl.gov

On the front cover:

The High Flux Isotope Reactor at Oak Ridge National Laboratory is the highest flux reactor-based source of neutrons for research in the United States (Credit: Oak Ridge National Laboratory).

Disclaimer

This information was prepared as an account of work sponsored by an agency of the U.S. Government. Neither the U.S. Government nor any agency thereof, nor any of their employees, makes any warranty, expressed or implied, or assumes any legal liability or responsibility for the accuracy, completeness, or usefulness, of any information, apparatus, product, or process disclosed, or represents that its use would not infringe privately owned rights. References herein to any specific commercial product, process, or service by trade name, trade mark, manufacturer, or otherwise, does not necessarily constitute or imply its endorsement, recommendation, or favoring by the U.S. Government or any agency thereof. The views and opinions of authors expressed herein do not necessarily state or reflect those of the U.S. Government or any agency thereof.

Editors: Tiera Cate, Barney Hadden

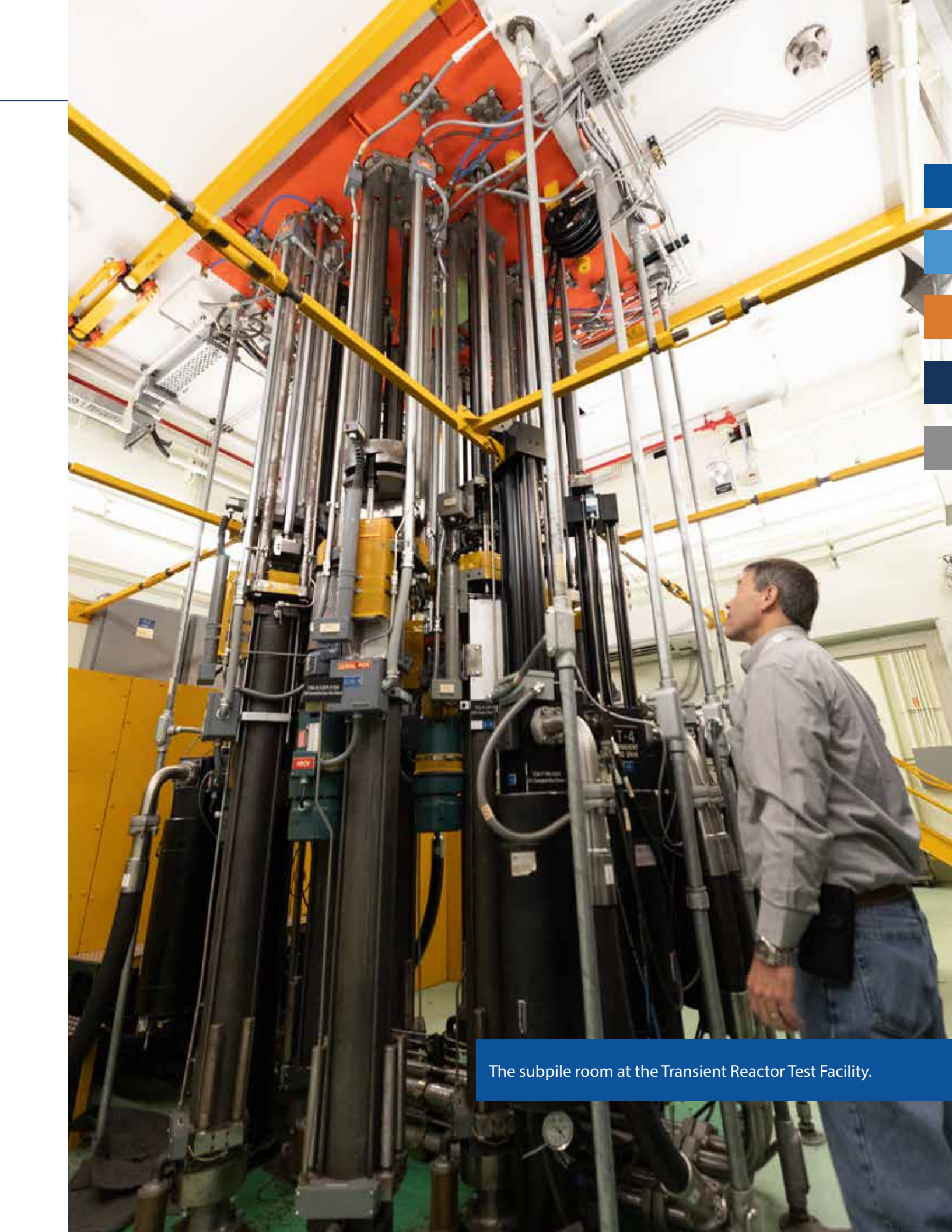
Writers: Tiera Cate, Alexis Starks, Paul Mesner Graphic Designers: Vanessa Godfrey, Kristyn St. Clair

TABLE OF CONTENTS

Nuclear Science User Facilities	
Our NSUF Program Office Team	6
From the Director	8
NSUF Overview	
NSUF by the Numbers	10
NSUF Across the Nation	12
Facilities and Capabilities	14
Highlights from the Year	16
Capability Updates	20
High-Performance Computing	22
MFC Remote Operating Capabilities	24
University of Texas at Austin Capabilities	26
The Nuclear Fuels and Materials Library	28
• Welcoming the New NSLIE Chief Scientists	30

CONTENTS

NSUF Awarded Projects - Irradiation Influence on Alloys Fabricated by Powder Metallurgy and Hot Isostatic Pressing for Nuclear Applications46 - X-ray Diffraction Tomography Analysis of SiC Composite Tubes Neutron-Irradiated with a Radial High-Heat Flux60 - *In situ* TEM Studies on Thermodynamic Stability and Microstructural Evolution of Zirconium Hydrides in Irradiation and Thermal Environments......64 - Irradiation Behavior of Nanostructured Ferritic/Martensitic Grade 91 Steel at High Dose......66 - Micromechanical Testing of LWR-Irradiated Harvested Reactor Internals70 - Irradiation Effects on Microstructure and Mechanical Properties in a Laser Welded ODS Alloy72 - Examining Microstructures and Mechanical Properties of Neutron and Ion Irradiated T91, HT9 and Alloy 800H74 - Neutron Irradiation Effects on the Tensile Properties of - Hydrogen-Retention of Yttrium Hydride under High-Temperature Proton Irradiation82 Resources NSUF List of Acronyms......86 NSUF Index......88



OUR NSUF PROGRAM OFFICE TEAM



Brenden Heidrich, Ph.D. Director (208) 526-8117 brenden.heidrich@inl.gov

Collin Knight Deputy Director (208) 533-7707 collin.knight@inl.gov



Jeff Benson Rapid Turnaround **Experiment Administrator** (208) 526-3841 jeff.benson@inl.gov





Kelly Cunningham Nuclear Fuels and Materials Library Coordinator (208) 526-2369 kelly.cunningham@inl.gov

Lindy Bean

(208) 526-4662 lindy.bean@inl.gov

Consolidated Innovative

Nuclear Research Administrator

Matt Anderson High-Performance Computing Manager (208) 526-4104 matthew.anderson2@inl.gov



Matthew Arrowood Experiment Manager (208) 526-3527 matthew.arrowood@inl.gov

Leigh Astle Experiment Manager (208) 526-1154 leigh.astle@inl.gov





Megan Broadhead Planning and Financial Controls Specialist (208) 526-7219 megan.broadhead@inl.gov

Tiera Cate Communications Liaison (208) 526-4828 tiera.cate@inl.gov





Michael Heighes Mechanical Properties Technical Lead (208) 526-1785 michael.heighes@inl.gov

Travis Howell Experiment Manager (208) 526-3817 travis.howell@inl.gov





Keith Jewell, Ph.D. Chief Scientist (208) 526-3944 james.jewell@inl.gov

Kip Kleimenhagen Experiment Manager (208) 526-8984 kip.kleimenhagent@inl.gov





William McClung Project Scheduler william.mcclung@inl.gov

Shane Oliverson Planning and Financial Controls Specialist (208) 526-5384 shane.oliverson@inl.gov





Simon Pimblott, D. Phil Chief Post Irradiation Scientist (208) 526-7499 simon.pimblott@inl.gov

Anna Podgorney Rapid Turnaround Experiment Administrator (208) 526-2123 anna.podgorney@inl.gov

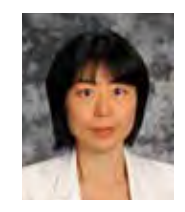




Aaron Russell *Experiment Manager*(208) 526-6984 *aaron.russell@inl.gov*

Trevor Smuin Experiment Manager (208) 526-5236 trevor.smuin@inl.gov





Rongjie Song Chief Scientist (208) 526-5117 rongjie.song@inl.gov

Madison Tippet Experiment Manager (208) 526-8984 madison.tippet@inl.gov





Renae Tripp Administrative Assistant (208) 526-6918 renae.tripp@inl.gov

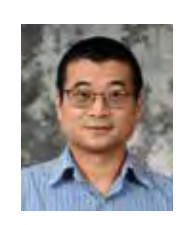
Dain White Technical Lead Software Engineer (208) 533-8210 dain.white@inl.gov





Eric Whiting
Director of High
Performance Computing
(208) 526-1433
eric.whiting@inl.gov

Peng Xu, Ph.D. Industry Program Lead (208) 533-8163 peng.xu@inl.gov





Alina Zackrone Post Irradiation Examination Experiment Manager (208) 526-6086 alina.zackrone@inl.gov

DIRECTOR



Brenden Heidrich, Ph.D.
Director
(208) 526-8117
brenden.heidrich@inl.gov

I am happy to be able to close out a successful first year in my role as the NSUF director. We were able to build upon the legacy that Todd Allen and Rory Kennedy built for NSUF, combined with strong support from the Department of Energy, Office of Nuclear Energy (DOE-NE). The program has had a consistent budget for the last few years, one that enabled us to carry out our mission and serve our users. Credit for our success belongs to our excellent team in the Program Office at Idaho National Laboratory and to our 20 partners across the U.S. I also wanted to thank Federal Program Manager Christopher Barr, who has been an invaluable connection to DOE-NE leadership. Dr. Barr has a background in many of the technical areas important to NSUF, making him a perfect fit for our program.

In addition to staff changes that happened last year, we also had our longtime colleague Jeff Benson move into the University Partnerships Office at INL. He was replaced in his role of Rapid Turnaround Experiment (RTE) lead by Anna Podgorney. Our communications lead, Tiera Cate took a position in INL's Diversity,

Equity, and Inclusion Office, and Alexis Starks has transitioned into that role in the Program Office. Finally, our financial specialist, Megan Broadhead, was replaced by Shane Oliverson. In the area of irradiation testing, Kip Kleimenhagen and Madison Tippet took over many of INL's irradiation experiments at the Transient Reactor Test Facility and the Advanced Test Reactor. We also had to replace the two NSUF chief scientists. I moved into the director's chair, and Dr. Simon Pimblott was appointed as an INL Laboratory fellow and moved to be the chief scientist for the Nuclear Science and Technology Directorate. We were fortunate to have many eager candidates and selected Dr. Keith Jewell and Dr. Rongjie Song to cover chief scientist duties.

The core of our program is the Competitive Access Award Program, both our short-term RTE and the multiyear Consolidated Innovative Nuclear Research (CINR) projects. Last year was the first since 2019 during which the NSUF was able to hold three full RTE calls. Over the year, we received 150 RTE proposals from our users and awarded 74 access projects. Our internal goal is

to maintain the award rate above 50% so that the user community can rely on RTEs to support their research and development efforts. We are planning to build upon this in 2024, adding a "Super-RTE" call that will allow larger-scope projects in a similar rapid format to accommodate user feedback gathered from across the community.

Similarly, 2023 was an excellent year for larger CINR projects. CINR is always changing to accommodate the needs of the nuclear-energy research and development community. In 2023, NSUF had two access-only topic areas in the CINR funding opportunity announcement. These didn't come with any research and development funding, but they still drew interest from university, industry, and national-laboratory researchers. Three CINR projects were awarded at a total cost over six million dollars, the highest amount since 2019. Working with our DOE-NE leadership, we were able to have both R&D and access-only topic areas for 2024.

We have also been involved in capability development and support for our user access projects. I believe that for a capability to be useful, it must represent a combination of three "P's": the physical infrastructure, the people trained to use it, and the procedures and processes to be able to carry out the work. NSUF makes small investments in the physical infrastructure, usually just filling in some small gaps to enable larger projects. We have been investing in the people through our

Instrument Scientist Program. Dr. Jeffrey Giglio oversees a group of NSUF instrument scientists, selected through a competitive process, who can be awarded up to 20% of their time to develop new capabilities and refine the procedures and processes at their instruments to support the NSUF users.

Our awarded research resulted in 114 peer-reviewed publications, bringing the NSUF total to 831 over our history. Perhaps more importantly, NSUF papers were cited 9,900 times, giving the program an H-Index of 44, up from 42 in 2022.

We were also able to increase our outreach efforts at conferences and professional meetings. NSUF participated in many conferences, supplying speakers and meeting users at expositions throughout the year. During these meetings, we realized that there were opportunities to expand our user community beyond our core audience. In 2024, we plan to attend a wider range of meetings in order to talk to new groups of potential users. We are also planning specific outreach to some underserved communities, minorityserving institutions, and other efforts to reduce burdens to accessing the user facility.

We had a great meeting with our user community in March at the Minerals, Metals & Materials Society conference in San Diego. Our audience totaled about 100 participants, split between in-person and online attendance. We also held an industry-engagement meeting in

collaboration with the Gateway for Accelerated Innovation in Nuclear Initiative at the Electric Power Research Institute's headquarters in Charlotte, North Carolina. We were able to meet with representatives from dozens of companies, both longstanding participants and new arrivals, in the nuclear-energy space. It is clear that the three pillars of our user community academia, industry, and national laboratories—have different needs and expectations for a user facility. In 2024, we will update our program's strategic plan, and feedback that we get from our users will be part of that.

In closing, I want to thank everyone—leadership, partners, and users—for their support over the last year. NSUF has never been in a better position to serve the nuclear-energy materials and fuels community. We are in the process of adding three new partners and rolling out new initiatives to support our users. Our High Performance Computing Team has developed a new tool to store and use NSUF project data. The Nuclear Fuels and Materials Library is adding materials from across the globe. You will see a lot of changes in the coming year. Stay tuned to our website and newsletter to be involved and informed.

Brenden

Brenden Heidrich, Ph.D. PE

NSUF BY THE NUMBERS

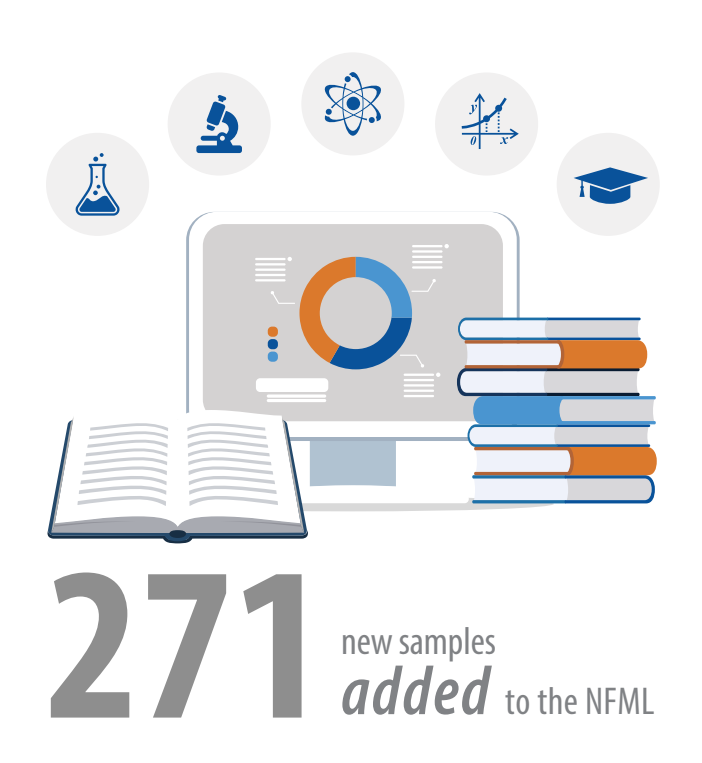
Note: Numbers for FY-23 only.

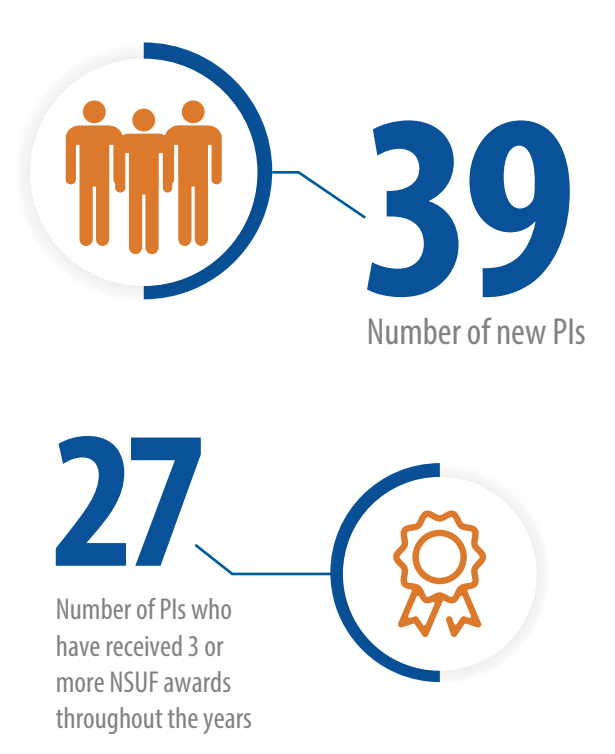


38 3% 3% 36% **58%** user Industry International National Universities institutions Organizations Laboratories received awards in FY-23

32) PERCENT

of projects involve a graduate student, either as a PI or a collaborator





NSUF ACROSS THE NATION







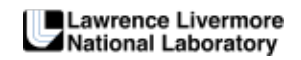






















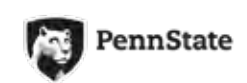


















NSUF User Institutions (FY-23)

Alabama

The University of Alabama in

Huntsville

California

KVA Stainless

University of California-Berkeley

University of California-Santa

Barbara

England

University of Manchester

Florida

Florida State University

University of Florida

Idaho

Center for Advanced Energy Studies

Idaho National Laboratory

Idaho State University

Univeristy of Idaho

llinois

Argonne National Laboratory

University of Illinois

Indiana

Purdue University

Japan

University of Tokyo

Kansas

Kansas State University

Maine

University of Maine

Maryland

Johns Hopkins University

United States Naval Academy

Michigan

University of Michigan

Missouri

Missouri Science and Technology

Nebraska

Univeristy of Nebraska-Lincoln

New Mexico

Los Alamos National Laboratory

Sandia National Laboratories

New York

General Electric Global Research

Rensselaer Polytechnic Institute

Stony Brook University

North Carolina

North Carolina State University

Ohio

The Ohio State University

Oregon

Oregon State University

Pennsylvania

Pennsylvania State University

Tennessee

Oak Ridge National Laboratory University of Tennessee-Knoxville

Texas

Texas A&M University

University of Texas at San Antonio

Washington

Pacific Northwest National Laboratory

Wisconsin

University of Wisconsin-Madison

FACILITIES AND CAPABILITIES

Partner Institution	Facilities					
Argonne National Laboratory	Intermediate Voltage Electron Microscopy (IVEM) Tandem Facility		√		√	
Brookhaven National Laboratory	National Synchrotron Light Source II					√
Center for Advanced Energy Studies	Microscopy and Characterization Suite (MaCS)		√			
Lawrence Livermore National Laboratory	Center for Accelerator Mass Spectrometry				√	
Los Alamos National Laboratory	Lost Alamos Neutron Scattering Center - Lujan Center Beamlines, Plutonium Surface Science Laboratory					√
Massachusetts Institute of Technology	Massachusetts Institute of Technology Nuclear Reactor, Massachusetts Institute of Technology Reactor	√	√			
North Carolina State University	PULSTAR Reactor	√				√
Oak Ridge National Laboratory	High-Flux Isotope Reactor, Irradiated Fuels Examination Laboratory, Irradiated Materials Examination and Testing Facility, Low Activation Materials Design and Analysis Laboratory	√	√	√		
The Ohio State University	The Ohio State University Research Reactor	✓		√		
Pacific Northwest National Laboratory	Materials Science and Technology Laboratory, Radiochemical Processing Laboratory		✓			

√	Neutron Irradiation	\checkmark	Ion Beam Irradiation
√	Post Irradiation Examination (PIE)	√	Characterization Beamline (Neutron, Positron,
√	Gamma Irradiation		or X-ray)

Partner Institution	Facilities					
The Pennsylvania State University	Radiation Science and Engineering Center	✓		√		/
Purdue University	Interaction of Materials with Particles and Components		√		√	
Sandia National Laboratories	Annular Core Research Reactor, SNL Ion Beam Laboratory, Sandia Pulse Reactor Facility Critical Experiment, Gamma Irradiation Facility	✓	√	√		
Texas A&M University	Accelerator Laboratory				√	
University of California, Berkely	Nuclear Materials Laboratory		√			
University of Florida	Nuclear Fuels and Materials Characterization		√			
University of Michigan	Irradiated Materials Testing Laboratory, Michigan Ion Beam Laboratory, Michigan Center for Materials Characterization		√		√	
The University of Texas at Austin	Nuclear Engineering Teaching Laboratory					√
University of Wisconsin	Characterization Laboratory for Irradiated Materials, University of Wisconsin Ion Beam		✓		√	
Westinghouse	Churchill Laboratory Services		✓			

FROM THE YEAR

In FY-23, the Nuclear Science User Facilities (NSUF) celebrated a year of remarkable achievements, marked by the timely completion of all major milestones, a significant augmentation of nearly 300 samples within the Nuclear Fuels and Materials Library, and the steadfast expansion of capabilities. Beyond these tangible advancements, the invaluable support from the Department of Energy's Office of Nuclear Energy remains the cornerstone of our research endeavors. As we navigate the complexities of nuclear material science, the collaboration and insights garnered from external perspectives underscore the vitality of our mission.

NSUF Hosts Partner Facilities Working Group, Capturing Input from Representatives

The NSUF team orchestrated a remarkable gathering, uniting minds from 20 partner facilities across national laboratories, universities, and industry. This assembly was the first partner meeting since 2017 and served as a formal platform to capture invaluable insights from NSUF partner facilities.

The collaborative spirit within NSUF and its expansive network of partners has fostered a nationwide infrastructure, allowing easier access to nuclear science research. At the heart of this convergence was a shared commitment to address the pressing challenges confronting today's reactor fleet, while charting a course for the reactors of tomorrow.

Throughout the gathering, discussions crackled with the



NSUF Director Brenden Heidrich welcomes partners to the Center for Advanced Energy Studies.

energy of innovation as participants exchanged ideas, experiences, and expertise. This fusion of minds sparked a symphony of innovative concepts, offering potential solutions to complex challenges and illuminating new pathways forward.

From enhancing reactor safety and efficiency to exploring advanced materials and fuel technologies, the spectrum of topics addressed underscored the breadth and depth of the collaborative effort.

By leveraging diverse perspectives

and interdisciplinary collaboration, participants paved the way for transformative advancements in the field.

As the meeting concluded, the echoes of collaboration lingered, leaving a mark on the future trajectory of nuclear science research. United by a shared vision and fueled by the passion for discovery, the NSUF and its partners stand poised to shape the future of nuclear science, driving innovation and progress for generations to come.



Industry Engagement Meeting Ignites Collaboration and Innovation

The NSUF Industry Engagement
Meeting convened in late September
at the Electric Power Research
Institute office in Charlotte, North
Carolina. The meeting was hosted in
a hybrid format that attracted more
than 50 participants, representing
25 organizations. The primary
objectives of this gathering were
to disseminate crucial information
about the NSUF Program to industry,
gather valuable feedback from
stakeholders, and foster enhanced
collaboration within this sector.

Key discussions during the meeting revolved around identifying and addressing barriers that hinder industry participation in the NSUF proposal process. Participants actively engaged in proposing potential solutions to overcome these obstacles. Significant focus was placed on the comprehensive exploration of material harvesting from decommissioned nuclear power plants, a critical topic that elicited in-depth deliberations.

Of particular note was insightful information shared regarding the Nuclear Fuels and Materials Library. This resource proves highly beneficial during the conclusion of irradiation and post-irradiation examinations, eliminating the need for users to dispose of irradiated materials. Additionally, any unused samples are seamlessly incorporated into the library, further enhancing its practical utility by ensuring their availability for future researchers.

Unlike alternative avenues that exclusively emphasize irradiation, the NSUF stands out by offering a holistic program encompassing both irradiation and post-irradiation examination. This approach underscores the program's commitment to providing a comprehensive and valuable experience for industry users.

The outcomes of the meeting were summarized, and a list of action items was compiled. These initiatives are geared towards providing robust support for industry users, reinforcing the NSUF's commitment to fostering innovation and collaboration within the nuclear industry.

Empowering Nuclear Materials Research at the Activated Materials Laboratory

By Alexis Starks

Last year, NSUF welcomed a new addition to the nuclear materials community. The Activated Materials Laboratory (AML), a new radiological facility at Argonne National Laboratory's Advanced Photon Source (APS), has recently been developed to assist the examination of radioactive samples at the High-Energy X-ray Microscope and other APS beamlines

In November 2023, Argonne National Laboratory and NSUF hosted a workshop at the new facility to introduce upgraded capabilities and showcase applications of high-energy X-rays in nuclear materials research and other fields. The workshop also helped researchers identify suitable X-ray techniques for such critical problems as understanding the effect of irradiation on structural- and cladding-materials performance, understanding environmental degradation mechanisms of materials, understanding transient behavior



Workshop participants on a tour of the High-Energy X-ray Microscope beamline (under construction), presented by Peter Kenesei (Credit: Argonne National Laboratory).

of fuels and fuel performance, and improving and validating computer models with critical experimental data from *in situ* and/or three-dimensional (3D) measurements at multiple length scales.

As an NSUF partner facility, the AML is motivated by the strong and growing interest in using advanced synchrotron techniques, particularly non-destructive high-energy X-rays, to study activated samples. The facility is capable of receiving/shipping, encapsulating, surveying, and transporting active samples. Materials will include common nuclear-reactor materials and fuels

in solid form, such as irradiated Febased alloys, Ni-based alloys, Zr alloys, refractory metals, ceramics, uranium, and uranium alloys. The AML also supports beamline experiments with dedicated equipment for *in situ* and/ or 3D studies.

The U.S. Department of Energy's NSUF program funds the AML's construction and operation. User access to the AML and the associated APS beamlines is expected to start in the fall of 2024, following the commissioning of the APS upgrade project.

Bridging Traditions through Research: The Ohio State University and the University of Michigan

In the realm of college football, few rivalries ignite passion of the game between the Ohio State University and the University of Michigan. This year, as the two powerhouse teams clashed undefeated, the anticipation leading up to their annual face-off reached a fever pitch. At OSU, students adorned the campus with a red "X" over every letter "M" as a jab at their rivals from Michigan. Meanwhile, across the border, Michigan fans dubbed the week leading up to the game as "hate week," adding fuel to the fiery rivalry.

Amidst this spirited competition, an unlikely alliance emerged – not on the football field, but in the pursuit of knowledge. Enter the NSUF, a catalyst for collaboration that transcends rivalries and united researchers from the Ohio State University and the University of Michigan in a shared quest for scientific discovery.

In a groundbreaking experiment led by Dr. Igor Jovanovic, director of the Neutron Science Laboratory and Applied Nuclear Science Instrumentation Laboratory at the University of Michigan, and Dr. Raymond Cao, director of the Nuclear Research Laboratory at the Ohio State University, traditional rivalries took a backseat to the pursuit of knowledge.

The experiment focused on studying low-energy nuclear recoils in germanium by leveraging state-of-the-art digitizers and electronics to



Dr. Cao and Dr. Jovanovic shaking hands (Credit: The Ohio State University).

achieve unprecedented sensitivities. From February 8, 2023, to November 8, 2023, Jovanovic's rapid-turnaround experiment was executed flawlessly, both on time and within budget.

Dr. Cao expressed enthusiasm about the collaborative effort, stating that "The OSU/Michigan rivalry has a long tradition, but under the NSUF, we are sharing the OSU research reactor with Michigan faculty and students to support their impactful research. We are forging a new OSU/Michigan nuclear tradition."

The irradiation campaign proved highly successful, thanks to the expert assistance of the Ohio State University reactor team, who facilitated the acquisition of all desired data. While detailed analysis of the data remains ongoing, initial

results show great promise, hinting at potential breakthroughs in nuclear science.

Echoing Dr. Cao's sentiments, Dr. Jovanovic emphasized the value of collaboration, remarking that "this has been a tremendous opportunity for my students. We have greatly enjoyed all of our previous collaborations with the OSU reactor laboratory and look forward to future OSU/Michigan research endeavors."

In the pursuit of knowledge, boundaries dissolve and rivalries take a backseat to the great goal of advancing science. Through initiatives like the NSUF, institutions once divided by tradition find common ground, proving that even the fiercest of rivals can come together in the name of research.

UPDATES

Making Research Accessible: The Nuclear Research Data System



The Nuclear Research Data System site is a public science data gateway that will allow public data to be downloaded, previewed, or enhanced through Al.

The Nuclear Research Data System (NRDS) provides public access to data in the emerging era of data science and explosive growth in artificial intelligence (AI). At a time when many public datasets are being locked behind paywalls or restricted-access sites, NRDS takes the opposite approach while also colocating dataset storage with highperformance computing resources to reduce the movement of data. This approach anticipates that nuclear data science and curation needs will continue to significantly outpace the capacity to move large amounts of data over large distances in the coming years. With its recent public release in December of 2023, the system promises to enable access to invaluable scientific data, ushering in a new era of exploration and innovation.

The foundation of NRDS is built upon the FpAIRe data-science principles: data should be findable, peekable, accessible, interoperable, reusable, and extensible. Each facet of this framework drives the design for nuclear-energy data-science curation.

Findability

Data should be easily findable and referenceable. Implementations of this principle include the use of digital object identifiers (DOI), tags, hierarchical data traversal, and Aldriven search.

Peekability

Peekability, the sibling of findability, offers a glimpse into a dataset that may too large or too difficult to view without downloading. Thumbnail images are the most common implementation of this principle. Peekable datasets reduce the unnecessary movement of data to save both time and energy.

Accessibility

Accessibility is core to data science and innovation. With neither passwords nor paywalls required for downloads, and a commitment to the Creative Commons Attribution license, NRDS embraces the spirit of openness, inviting researchers from every corner of the globe to partake in the pursuit of scientific engagement.

Interoperability

Interoperability in datasets ensures the longevity of the dataset.
Open-source formats are easily interoperable with multiple analysis tools, while proprietary formats are not generally interoperable and die when the controlling vendor discontinues support.

Reusability

Reusability lies at the heart of NRDS, where data can find new life beyond individual projects. Stored in a non-proprietary format within the vast expanse of high-performance-computing storage, data within NRDS becomes a timeless repository of collective wisdom.

Extensibility

Al and data-science analysis serve to extend a dataset, with metadata that can become as valuable as the original dataset. Data naturally become extensible as they accommodate the exponential advances in machine learning and Al. Extensibility breathes new life into data, infusing them with the transformative power of annotation and AI analysis, which unveil hidden insights and pave the way for groundbreaking discoveries.

NRDS exemplifies the NSUF commitment to open science and innovation in nuclear-energy research and supports a renaissance in nuclear energy, driven by advances in data science.

COMPUTING



The Sawtooth supercomputer at INL.

Our Supercomputers

Sawtooth:

Sawtooth is an HP SGI 8600-based system with 99,792 cores, 99,792 TB of memory and a LINPACK rating of 5,600 TFlop/s. Sawtooth's network is an enhanced hypercube, utilizing EDR/HDR InfiniBand. Individual compute nodes contain dual Xeon Platinum 8268 processors with 24 cores each and a total of 192 GB of memory. Some nodes also have 4 NVIDIA V100 GPUs and an additional 192 GB of RAM for a total of 384 GB of memory. Sawtooth came online in Fall 2019 and ranked 37 on the November 2019 TOP500 list.

Lemhi:

Lehmi is a Dell 6420-based system with 20,160 cores, 20,160 TB of memory and a LINPACK rating of 1,000 TFlop/s. Lemhi's network is an Omni-Path fat tree. Individual compute nodes contain dual Xeon Gold 6148 processors with 20 cores each and a total of 192 GB of memory. Lemhi came online in Fall 2018 and ranked 427 on the November 2018 TOP500 list.



Hoodoo:

Hoodoo is a Lambda Hyperplane deep-learning distributed-memory system with 44 NVIDIA A100 Tensor Core GPUs and 7.2 TB of total memory, dedicated to machine-learning applications. Hoodoo provides a maximum GPU performance of 429 TFlop/s double precision or 858 TFlop/s single precision.



Viz:

The Viz cluster has five compute nodes. Two compute nodes have 24 cores with 775 GB of memory, one has 16 cores with 251 GB of memory, one has 12 cores with 251 GB of memory, and the final one has 12 cores with 125 GB of memory. The nodes have either four NVIDIA Quadro M6000 GPUs with an additional 24 GB of RAM or two NVIDIA Quadro RTX6000 GPUs.



High-Performance Computing Utilization

Total Million Core Hours



64.3%

National Laboratory



26% University



8.6% Industry



1.1% Other

CAPABILITIES



The Research Collaboration Building serves as a landing spot, collaborative working space, and training area for a growing number of students, visiting researchers, and postdoctoral researchers engaged in work at MFC.

Outside looking in: Remote capabilities at the Research Collaboration Building improve ease of research

By Paul Menser

The Research Collaboration Building at Idaho National Laboratory's Materials and Fuels Complex (MFC) now offers remote operating system capabilities. This enhancement provides researchers with easier access to select instruments within the Irradiated Materials Characterization Laboratory (IMCL), a key resource for high-demand instruments such as the plasma focused ion beam and transmission electron microscopes.

Completed in 2019, the building features 28 offices for researchers, staff members, and long-term visitors. It contains 23 workstations and five collaboration spaces where scientists can host research partners and analyze data together. The inclusion of remote consoles enables after-hours access

to IMCL's advanced microscopes, offering scheduling flexibility and significantly increasing the available hours on the instruments in IMCL.

Grace Burke, a world-leading researcher in advanced microstructural characterization and irradiation embrittlement, expressed the tremendous advantage of remote microscope use for research and teaching purposes. Burke, who became a Laboratory Fellow in March, had her first experience with remote operation at INL, and spoke highly of the capability. She leads INL's research on reactor structural materials and actively promotes education in electron microscopy and nuclear materials research.

Burke emphasized the benefits of remote capabilities. "Microscope rooms can be on the small side, making it difficult to have additional people in the room when you would like to demonstrate specific techniques or share tips on optimizing analytical conditions," she said. With this capability, "it's possible to actually take control of the microscope, and if a colleague is involved with the research, you can share the session, maximizing efficiency as well as providing guidance on technique optimization.



The IMCL remote console allows researchers to operate the IMCL remotely, improving utilization, reducing operations costs, and increasing overall access.

If you're performing a very long data acquisition experiment, this allows you to multitask and work on other things while keeping an eye on the specimen."

According to Colin Judge, division director of Characterization and Post-Irradiation Examination, the purpose of remote access is to improve instrument utilization, reduce operation costs, and provide increased access for after-hours and weekend work. It enhances data security, resiliency, and access to high-performance computing resources. Because the capability exists outside MFC's secured perimeter, it eliminates the need for researchers to undergo the training and protocols required for an actual visit to IMCL. With reduced risk of contamination and minimized training requirements since physical access to IMCL is not necessary,

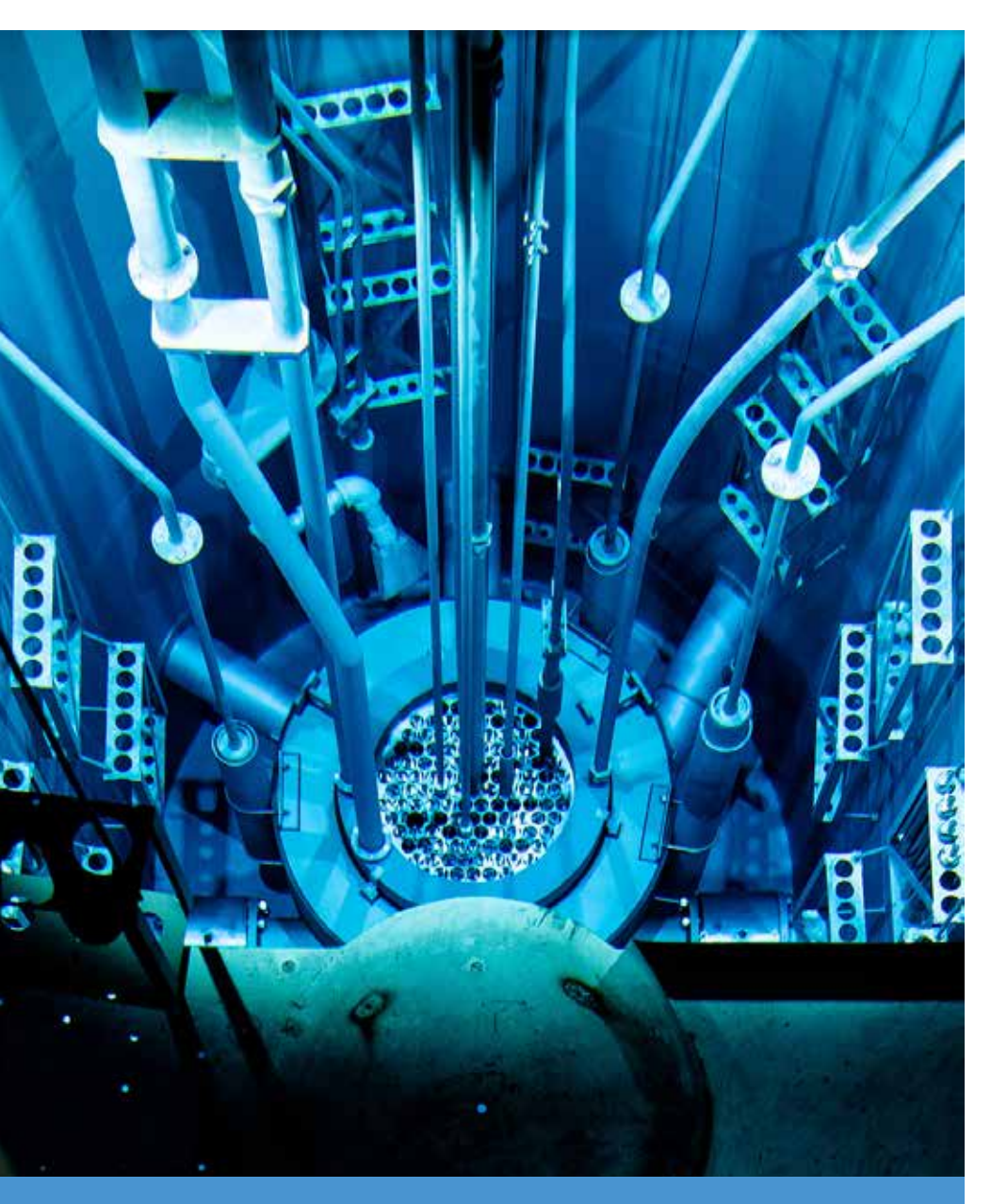
remote capabilities especially benefit radiological workers and researchers.

The development of these capabilities received support from MFC's management team. It was a collaborative effort among the Advanced Characterization, IMCL Facility Operations, and the Computer Engineering departments. The Nuclear Science User Facilities has been supporting the construction of the Research Collaboration Building since FY-18 and recently provided funding to acquire software to enable remote access to the Transmission Electron Microscope in IMCL.

According to Tiankai Yao, group lead for INL Materials Characterization and Informatics, this achievement and data centralization led by Fei Xu represents Phase One of the project. Phase Two aims to extend remote accessibility of the microscopes to researchers at INL's Research and Education Campus in Idaho Falls. Yao explained that this expansion would involve collaboration with the MFC computer engineering department and lab's information management experts to ensure safe data distribution.

The integration of remote operating system capabilities within the Research Collaboration Building stands as a transformative milestone in advancing research accessibility and collaboration. This was achieved through collaborative efforts across various departments, and marks the successful completion of Phase One of this initiative. This ongoing project demonstrates a commitment to innovation, heralding a future of enhanced research methodologies and broader collaboration in the scientific community.

CAPABILITIES



UT-Austin's 1.1 MW TRIGA Mark II reactor (Credit: University of Texas at Austin).

The University of Texas at Austin Joins NSUF to Advance Nuclear Science

In the realm of nuclear science, collaboration is vital to unlocking new frontiers of knowledge and innovation. This sentiment rings especially true with the recent addition of the University of Texas at Austin's Prompt Gamma Ray Activation Analysis Facility (PGAA) to the roster of partners within the Nuclear Science User Facilities (NSUF).

Nestled within the Nuclear Engineering Teaching Laboratory (NETL) at UT-Austin lies a 1.1 MW TRIGA Mark II reactor that achieved initial criticality in 1992. Designed primarily as a neutron-beam facility, this reactor houses a state-of-theart PGAA system, complete with a cold neutron source, setting a new standard for precision in nuclear analysis.

The NETL's offerings extend far beyond its reactor capabilities. With additional radiation sources that include a Thermo MP320 14-MeV neutron generator, Pu(Be) and Cf-252 neutron sources, and calibrated alpha-, beta-, and gamma-radiation sources, this laboratory is a playground for nuclear researchers.

Within its analytical laboratories, researchers have access to myriad specialized facilities, from the Radiation Effects and Detector Development Laboratory to the Radioactive Experiment and Radiochemistry Laboratory. These facilities provide the infrastructure necessary to conduct a wide range of experiments, from neutron activation analyses to gamma-ray spectroscopy.

Moreover, the NETL is at the forefront of nuclear and applied robotics, developing and deploying advanced robotic systems to

navigate hazardous environments and minimize risk to human operators. This commitment to safety and innovation underscores UT-Austin's dedication to pushing the boundaries of nuclear research.

The crown jewel of the NETL, however, remains its PGAA system, which has been in operation for over two decades. It has evolved into an analytical instrument capable of providing precise measurements for a variety of elements in bulk samples. Notably, the system's background radiation levels are among the lowest in the United States— a testament to its sophistication and precision.

Collaborations between UT-Austin and the NSUF are positioned to yield groundbreaking discoveries. They include a shared commitment to excellence, innovation, and collaboration.



The Nuclear Engineering Teaching Laboratory's 1.1MW TRIGA research reactor (Credit: University of Texas).

THE NUCLEAR FUELS AND MATERIALS LIBRARY



The Center for Advanced Energy Studies located on the Research and Education Campus in Idaho Falls.

Curating the Future of Nuclear Research: The Nuclear Fuels and Materials Library

In the world of nuclear energy research, the quest for innovation and advancement relies heavily on access to high-value irradiated fuel and material samples. At the forefront stands the Nuclear Fuels and Materials Library (NFML), a beacon of knowledge owned by the United States Department of Energy Office of Nuclear Energy (DOE-NE). The library is meticulously curated by the Nuclear Science User Facilities (NSUF). This archive represents the largest global repository of its kind, housing samples and technical insights gleaned from past and ongoing irradiation test campaigns.

From its humble beginnings with approximately 3,500 samples in FY-15, the NFML has burgeoned into a repository boasting over 9,000 samples, all cataloged and accessible through the NSUF database. However, the NFML is more than just a repository. It's a testament to the collaborative spirit of the nuclear research community, bridging the gap between academia, industry, and government initiatives.

One of the NFML's most crucial roles is its ability to rescue valuable materials that might otherwise face disposal as waste or languish in long-term storage. Through partnerships with decommissioned power reactors and donations from various sources, the NFML ensures that these materials find new life as vital resources for nuclear researchers.



The Center for Advanced Energy Studies located on the Research and Education Campus in Idaho Falls.

FY-23 marked a significant occasion for the NFML, culminating in the attainment of a Level II milestone, based on the transfer of the Ki-Jang Research Reactor Lead Test Fuel Assemblies. This is a testament to the NFML's growing influence within the nuclear research community. Ongoing efforts included the procurement of samples irradiated in the NSUF-designed small standard capsule, laying the groundwork for future breakthroughs in nuclear science.

Perhaps the most compelling aspect of the library lies in salvaging irradiated material from decommissioned nuclear power plants. Despite logistical challenges and funding constraints, NSUF staff continued a relentless pursuit, forging partnerships with likeminded organizations in the US, the UK, and the EU to ensure the NFML remains the repository of choice for these invaluable materials.

The NFML's presence in collaborative meetings with national laboratories, regulatory bodies, and industry stakeholders underscores its pivotal role in shaping the future of nuclear research. Through initiatives like the NSUF data management plan, the NFML remains committed to transparency and accessibility, laying the groundwork for a future

where research data are shared openly and responsibly.

As NFML enters FY-24, its legacy as the foremost archive of nuclear research samples and materials is firmly cemented. With each new addition to its inventory and every successful collaboration, the NFML paves the way for a brighter future in which nuclear power stands as a safe, cost-effective, and sustainable energy solution.

CHIEF SCIENTISTS



Keith Jewell

Keith Jewell is an invaluable chief scientist for the Nuclear Science User Facilities (NSUF). For Jewell, the decision to pursue nuclear science was rooted in a passion for physics since high school. However, it was during graduate school that he stumbled upon accelerator-based experimental nuclear physics, which sparked his interest in nuclear science.

Immediately after graduate school, Jewell joined Idaho National Laboratory. Initially focused on gamma ray spectroscopy and actinide cross-section measurements, he later diversified into areas like national security and instrumentation development. This journey eventually led him to the NSUF, where he served as one of the primary technical leads for large Consolidated Innovative Nuclear Research projects. This gave him

the necessary experience for the irradiation chief scientist position.

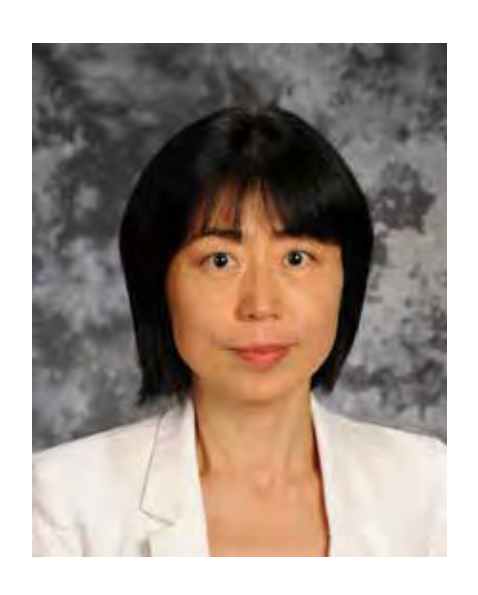
His advice for aspiring scientists in the field is straightforward: "Grab hold and run with it as quickly as possible. The enthusiasm for nuclear science, expressed in opportunity and funding, has never been this good. It's such a wonderful time to be part of the nuclear science research community."

As one of our chief scientists, Jewell values the variety of projects and collaborations that NSUF offers, providing constant opportunities for learning and growth. "I'm so lucky to have the variety of different projects and the wide range of interactions with other researchers from universities, industry, and national laboratories," said Jewell. "Every project has unique components and new perspectives. It's very much a position where I can continue learning."

Recognizing the importance of inclusivity and diversity in advancing nuclear science, Jewell also highlights his excitement and pride in the efforts NSUF is making to engage small colleges and universities. Looking ahead, he sees NSUF's work as crucial to meeting the world's energy needs, especially in terms of reducing carbon emissions and supporting emerging nations.

"We know the need and demand for nuclear energy is a critical part of any long-term solution to meet the energy needs of the world," said Jewell. "NSUF, because it isn't tied to any particular program, has the flexibility and the creativity to allow research in low technology readiness level technologies and ideas that could lead to gamechanging advances in the nuclear energy efforts."

With each endeavor, Keith Jewell and the NSUF pave the way for transformative advancements, propelling humanity toward a brighter, more sustainable future powered by nuclear innovation.



Rongjie Song

Rongjie Song, the NSUF's esteemed post-irradiation chief scientist, brings a wealth of experience and expertise garnered over a dynamic career, that spans multiple industries. With a background deeply rooted in physical metallurgy, materials science, and engineering, Song's journey into the realm of nuclear science was propelled by a desire to harness the potential of clean energy and innovative industrial processes.

Prior to her tenure at INL, Song dedicated 12 years to research and development in the steel industry, honing skills in alloy design, industrial processing, microstructural characterization, mechanical testing, and materials qualification. Song's passion for understanding the intricate interplay between composition, microstructure, and mechanical properties paved the way for her transition into the nuclear arena.

The allure of NSUF's mission—providing researchers access to cutting-edge capabilities for advancing nuclear energy technologies—resonated deeply with Song. Her expansive knowledge in materials, advanced characterization, testing, and qualification found a natural synergy with NSUF's objectives, propelling her into a pivotal role within the program.

When asked about her inspiration for pursuing a career in nuclear science, Song's conviction was palpable. "I see a lot of potential in nuclear energy," she shared. "It's a zero-emission clean-energy source with the capacity to revolutionize industrial processes and mitigate environmental impacts." Her pride in contributing to a cleaner, healthier future through nuclear science and technology is evident, fueled by the knowledge that her work plays a crucial role in reducing harmful air pollutants and advancing societal well-being.

As the post-irradiation chief scientist, Song enjoys the opportunities that the NSUF provides, "I can aid and provide leadership in the identification, evaluation, development, and execution of NSUF projects in collaboration with university, industry, national-laboratory, small-business, and international users." The role is not just about advancing scientific knowledge, but also about fostering collaboration and innovation to address the nation's energy challenges.

In line with NSUF's commitment to education and outreach, Song aids in efforts such as the NSUF Minority Serving Institution Initiative. This project aims to increase the visibility and accessibility of NSUF resources to professors and students from underrepresented communities, empowering them with scientific instrumentation and professional-development opportunities. Through initiatives like these, NSUF not only expands its scientific outreach, but also cultivates a diverse and inclusive community dedicated to advancing nuclear science and technology.

In the hands of Jewell, Song, and their esteemed colleagues, the NSUF continues to illuminate the path toward a sustainable nuclear future, guided by innovation, collaboration, and an unwavering dedication to shaping tomorrow's world, today.

PROJECTS

Awarded Consolidated Innovative Nuclear Research Projects FY-23

Project Title	PI Organization	NSUF Facilities
Irradiation-Corrosion of Alumina- Forming Austenitic Stainless Steels in Static Lead	Janelle Wharry Purdue University	Post-Irradiation Examination Using High-Flux Isotope Reactor, Low Activation Materials Design and Analysis Laboratory at Oak Ridge National Laboratory; Sample Preparation and Shipping Using Interaction of Materials with Particles and Components Testing at Purdue University
UN Multi-design Irradiation Campaign: A Critical Assessment of Accelerated Burnup and Main Correlations for Mechanistic Fuel Performance Modeling	Elizabeth Sooby University of Texas at San Antonio	Post-Irradiation Examination Using High-Flux Isotope Reactor, Low Activation Materials Design and Analysis Laboratory at Oak Ridge National Laboratory
Investigation of Intergranular Cracking of Highly Irradiated Austenitic Stainless Steels—Materials of Pressurized Water Reactors—In Ambient Conditions	Maxim Gussev Oak Ridge National Laboratory	Post-Irradiation Examination Using Low Activation Materials Design and Analysis Laboratory at Oak Ridge National Laboratory; Sample Irradiation Using Michigan Ion Beam Laboratory at University of Michigan; Sample Preparation and Shipping Using Churchill Laboratory Services at Westinghouse



Rapid Turnaround Experiment (RTE) Projects Awarded FY-23 First Call

Project Title	PI Organization	NSUF Facilities
Compositional and Defect Analysis of the FCCI in High Burnup UO_2	Allison Probert University of Florida	Post-Irradiation Examination Using Irradiated Fuels Examination Laboratory, Low Activation Materials Design and Analysis Laboratory at Oak Ridge National Laboratory
Elucidating the Effect of Radiation- Induced Defect Accumulation on Swelling in UN Using <i>in situ</i> TEM Irradiation	Caitlin Kohnert Los Alamos National Laboratory	Post-Irradiation Examination Using Intermediate Voltage Electron Microscopy (IVEM)-Tandem Facility at Argonne National Laboratory
Evolution of Dispersoid in Austenitic Fe-Cr-Ni Oxide Dispersion Strengthened Alloy in Ion Irradiation	Ching-Heng Shiau Center for Advanced Energy Studies	Post-Irradiation Examination Using Microscopy and Characterization Suite at Center for Advanced Energy Studies; Sample Irradiation Using Accelerator Laboratory at Texas A&M University
Assessment of Local Thermal Conductivity and Microstructure of Irradiated U-20 wt% Pu-10 wt% Zr Alloy	Cynthia Adkins Idaho National Laboratory	Post-Irradiation Examination Using Irradiated Materials Characterization Laboratory at Idaho National Laboratory
Neutron Irradiation of Updated In-Pile Steady State, Extreme Temperature Experiment (INSET)	Emily Hutchins University of Tennessee- Knoxville	Sample Irradiation Using Ohio State University Research Reactor at the Ohio State University
Neutron Irradiation of a Radiation Resistant Digitizer at PULSTAR	Frederick Reed Oak Ridge National Laboratory	Sample Irradiation Using Nuclear Reactor Program PULSTAR at North Carolina State University
<i>In situ</i> Mechanical Testing of Irradiated Zr Single Crystals	Geoffrey Beausoleil Idaho National Laboratory	Sample Preparation and Shipping Using Irradiated Materials Characterization Laboratory at Idaho National Laboratory; Sample Irradiation Using SNL Ion Beam Laboratory at Sandia National Laboratories
4D-STEM Strain Mapping of Radiation Induced Defects	Hi Vo Los Alamos National Laboratory	Post-Irradiation Examination Using Intermediate Voltage Electron Microscopy (IVEM)-Tandem Facility at Argonne National Laboratory
Measurement of 254-eV Nuclear Recoils in Germanium	Igor Jovanovic University of Michigan	Sample Irradiation Using Ohio State University Research Reactor at The Ohio State University

Project Title	PI Organization	NSUF Facilities
Effect of Neutron Radiation on Density and Mechanical Properties of White Cement Paste	Ippei Maruyama University of Tokyo	Post-Irradiation Examination Using Low Activation Materials Design and Analysis Laboratory at Oak Ridge National Laboratory
Irradiation of Radiation-Hard GaN Transistors for Mixed Gamma and Neutron Field under High Temperature	Jack Lanza The Ohio State University	Sample Irradiation Using Ohio State University Research Reactor at The Ohio State University
The Effect of Irradiation on the Densities of Chloride-Bearing Molten Salts	Joanna McFarlane Oak Ridge National Laboratory	Post-Irradiation Examination Using Massachusetts Institute of Technology Nuclear Reactor Laboratory at Massachusetts Institute of Technology
Spatially Resolved Thermal Conductivity Measurement of Medium Burnup MOX Fuel	Joshua Ferrigno The Ohio State University	Post-Irradiation Examination Using Irradiated Materials Characterization Laboratory at Idaho National Laboratory
Dual Ion Beam Irradiation and Post- Irradiation-Examinations of Alumina Coating on Stainless Steel	Junhua Jiang Savannah River National Laboratory	Post-Irradiation Examination Using Microscopy and Characterization Suite at Center for Advanced Energy Studies; Sample Irradiation Using Accelerator Laboratory at Texas A&M University
Investigation of Simultaneous Irradiation and Creep Behavior of Cr Thin Films	Kelvin Xie Texas A&M University	Post-Irradiation Examination Using Microscopy and Characterization Suite at Center for Advanced Energy Studies; Sample Irradiation Using Accelerator Laboratory at Texas A&M University
Deconvoluting Void and Bubble Effects on Deformation-Induced Martensitic Transformations in Austenitic Stainless Steel Using 4D STEM Strain Mapping	Keyou Mao Florida State University	Post-Irradiation Examination Using Microscopy and Characterization Suite at Center for Advanced Energy Studies; Sample Irradiation Using Accelerator Laboratory at Texas A&M University
Microstructural Characterization of Neutron Irradiated C-C Composites	Lee Margetts University of Manchester	Post-Irradiation Examination Using Low Activation Materials Design and Analysis Laboratory at Oak Ridge National Laboratory
High-Resolution Characterization of Neutron-Irradiated Cr-Fe-Mn-Ni-(Al, Ti) High-Entropy Alloys	Michael Moorehead Idaho National Laboratory	Post-Irradiation Examination Using Irradiated Materials Characterization Laboratory at Idaho National Laboratory

Project Title	PI Organization	NSUF Facilities
Microstructural Origin of Irradiation Hardening and Embrittlement in Irradiated Second Generation FeCrAl Alloys	Nathan Almirall General Electric Global Research	Post-Irradiation Examination Using Low Activation Materials Design and Analysis Laboratory at Oak Ridge National Laboratory
Ion Irradiation Tolerance of Gadolinium Titanates/Zirconates as Candidates for Waste Form Matrices	Nestor Zaluzec Argonne National Laboratory	Post-Irradiation Examination Using Intermediate Voltage Electron Microscopy (IVEM)-Tandem Facility at Argonne National Laboratory
Mesoscale Irradiation of HT-9	Peter Hosemann University of California-Berkeley	Sample Irradiation Using Center for Accelerator Mass Spectrometry at Lawrence Livermore National Laboratory; Post-Irradiation Examination Using Nuclear Materials Laboratory at University of California-Berkeley
Serial Sectioning to Quantify Fission Induced Microstructural Evolution in U-Zr Alloys	Walter Williams Idaho National Laboratory	Post-Irradiation Examination Using Irradiated Materials Characterization Laboratory at Idaho National Laboratory
Isotope Density Mapping Using Energy Resolved Neutron Resonance Imaging of a High Burnup UO2 Fuel Fragment	William Cureton Oak Ridge National Laboratory	Post-Irradiation Examination Using Los Alamos Neutron Scattering Center—Lujan Center Beamlines at Los Alamos National Laboratory
Electron Tomography Study of Dislocation Loops and Precipitates in Ion Irradiated Fe-Cr Alloys	Yajie Zhao University of Tennessee- Knoxville	Post-Irradiation Examination Using Low Activation Materials Design and Analysis Laboratory at Oak Ridge National Laboratory

Rapid Turnaround Experiment (RTE) Projects Awarded FY-23 Second Call

Project Title	PI Organization	NSUF Facilities
Recovery of Irradiated Tantalum, a Pre-Cursor to Understanding Ferritic (BCC) Steels	Aaron Kohnert Los Alamos National Laboratory	Sample Preparation and Shipping Using Hot Fuel Examination Facility at Idaho National Laboratory; Post-Irradiation Examination Using Los Alamos Neutron Scattering Center—Lujan Center Beamlines at Los Alamos National Laboratory
Correlating Microstructure to the Thermal Conductivity of Irradiated U-20Pu-10Zr Fuels	Allison Probert University of Florida	Post-Irradiation Examination Using Irradiated Materials Characterization Laboratory at Idaho National Laboratory

Project Title	PI Organization	NSUF Facilities
Critical Database Development of High Dose Microstructure Evolution in Irradiated Advanced Steels	Arthur Motta Pennsylvania State University	Post-Irradiation Examination Using Low Activation Materials Design and Analysis Laboratory at Oak Ridge National Laboratory
Mechanisms of Outstanding Radiation Tolerance in High Entropy Alloys with Nanoprecipitates	Boopathy Kombaiah Idaho National Laboratory	Post-Irradiation Examination Using Michigan Ion Beam Laboratory at University of Michigan
Quantifying the Effect of Simultaneous vs. Sequential Irradiation on Creep Performance of Additively Manufactured Austenitic Stainless Steel	Caleb Massey Oak Ridge National Laboratory	Post-Irradiation Examination Using Michigan Ion Beam Laboratory at University of Michigan
Investigation of Void Swelling and Chemical Segregation in Heavy Ion Irradiated Compositionally Complex Alloys	Calvin Parkin Sandia National Laboratories	Post-Irradiation Examination Using Microscopy and Characterization Suite at Center for Advanced Energy Studies
Understanding the Origin of Irradiation- Induced Yield Drop Phenomena in Grade 91	Donna Guillen Idaho National Laboratory	Post-Irradiation Examination Using Microscopy and Characterization Suite at Center for Advanced Energy Studies; Sample Preparation and Shipping Using Hot Fuel Examination Facility at Idaho National Laboratory
The Role of Nb and Impurities on Nano- Oxide Retention Neutron Irradiation	Elizabeth Getto United States Naval Academy	Post-Irradiation Examination Using Low Activation Materials Design and Analysis Laboratory at Oak Ridge National Laboratory
Stability of VN, TaN, and TaC MX-type Precipitates in Ferritic Steels Under Neutron Radiation	Emily Proehl University of Tennessee- Knoxville	Post-Irradiation Examination Using Low Activation Materials Design and Analysis Laboratory at Oak Ridge National Laboratory
Investigation of Evolution of Defects in $\beta\text{-Ga}_2\textbf{0}_3$ Under Irradiation and High Temperature	Ge Yang North Carolina State University	Post-Irradiation Examination Using Activated Materials Laboratory, Intermediate Voltage Electron Microscopy—Tandem Facility at Argonne National Laboratory
Investigating Nitrogen Effects on the Mechanical Properties and Microstructure Evolution in Neutron Irradiated HT-9 Steel	Hyosim Kim Los Alamos National Laboratory	Post-Irradiation Examination Using Irradiated Materials Examination and Testing Facility at Oak Ridge National Laboratory
Neutron Detection via Defects Created in Hexagonal Boron Nitride	James Edgar Kansas State University	Sample Irradiation Using Ohio State University Research Reactor at The Ohio State University

Project Title	PI Organization	NSUF Facilities
Measuring the Microstructural Changes and Elastic Properties of Oxidized Neutron-Irradiated Graphite	James Spicer Johns Hopkins University	Post-Irradiation Examination Using Low Activation Materials Design and Analysis Laboratory at Oak Ridge National Laboratory
Room Temperature Tensile Properties of ATR Neutron Irradiated T91	James Stubbins University of Illinois	Sample Preparation and Shipping Using Hot Fuel Examination Facility at Idaho National Laboratory; Post-Irradiation Examination Using Materials Science and Technology Laboratory at Pacific Northwest National Laboratory
Gas Bubble Superlattice Formation in Metals at Cryogenic Temperature and in Ceramics at High Temperature	Jian Gan Idaho National Laboratory	Post-Irradiation Examination Using Intermediate Voltage Electron Microscopy—Tandem Facility at Argonne National Laboratory; Sample Preparation and Shipping Using Irradiated Materials Characterization Laboratory at Idaho National Laboratory
<i>In situ</i> Synchrotron Radiation Diffraction Study of the Effect of Radiation Damage on the Precipitation and Dissolution of Hydrides in Zircaloy	Jonathan Balog Pennsylvania State University	Post-Irradiation Examination Using National Synchrotron Light Source II at Brookhaven National Laboratory
Hydrogen Quantification in Neutron Irradiated Monolithic Metal Hydrides Compacts	Lance Snead Stony Brook University	Post-Irradiation Examination Using Massachusetts Institute of Technology Nuclear Reactor Laboratory at Massachusetts Institute of Technology
In situ Irradiation of Uranium Carbide	Lingfeng He North Carolina State University	Sample Irradiation Using Intermediate Voltage Electron Microscopy— Tandem Facility at Argonne National Laboratory; Sample Preparation and Shipping Using Irradiated Materials Characterization Laboratory at Idaho National Laboratory
Investigating the Effect of Solute Segregation on Defect Recovery Kinetics in Reactor-Irradiated Ti	Michael Short University of Michigan-Ann Arbor	Post-Irradiation Examination Using Irradiated Materials Characterization Laboratory at Idaho National Laboratory; Sample Preparation and Shipping Using Massachusetts Institute of Technology Nuclear Reactor Laboratory at Massachusetts Institute of Technology
Atom Probe Characterization of HT-9 as a Function of Neutron Irradiation Temperature	Ramprashad Prabhakaran Pacific Northwest National Laboratory	Post-Irradiation Examination Using Microscopy and Characterization Suite at Center for Advanced Energy Studies; Sample Preparation and Shipping Using Materials Science and Technology Laboratory at Pacific Northwest National Laboratory
Increasing the Sensitivity of Passive SiC Thermometry through Nanocalorimetry Experiments	Stephen Taller Oak Ridge National Laboratory	Post-Irradiation Examination Using Michigan Center for Materials Characterization at University of Michigan

Project Title	PI Organization	NSUF Facilities
Post-Incubation Void Swelling in Tempered Martensitic Steels	Takuya Yamamoto University of California-Santa Barbara	Sample Irradiation Using Michigan Ion Beam Laboratory at University of Michigan
Correlative Atom Probe Tomography of the Buffer-IPyC Interlayer Region of TRISO-coated Particles	Tanner Mauseth Idaho State University	Post-Irradiation Examination Using Irradiated Materials Characterization Laboratory at Idaho National Laboratory
Effect of Ion Irradiation and Dose Rates on 316LY Oxide-Dispersion- Strengthened Steel Additively Manufactured by Laser-Directed Energy Deposition	Tianyi Chen Oregon State University	Post-Irradiation Examination Using Microscopy and Characterization Suite at Center for Advanced Energy Studies; Sample Irradiation Using Accelerator Laboratory at Texas A&M University
Irradiating a Novel Thin-Film Scintillator for Neutron Radiography	Zhibin Yu Florida State University	Sample Irradiation Using Ohio State University Research Reactor at The Ohio State University

Rapid Turnaround Experiment (RTE) Projects Awarded FY-23 Third Call

Project Title	PI Organization	NSUF Facilities
Testing of Ex-Core Monitoring Configurations at the Ohio State University Research Reactor (OSURR)	Angela Di Fulvio University of Illinois at Urbana-Champaign	Sample Irradiation Using Ohio State University Research Reactor at the Ohio State University
Proton Irradiation of High Entropy Carbide Ceramics	Bai Cui University of Nebraska- Lincoln	Post-Irradiation Examination Using Irradiated Materials Characterization Laboratory at Idaho National Laboratory; Sample Irradiation Using Michigan Ion Beam Laboratory at University of Michigan
Characterization of the Total-Dose Effect on State-of-the-Art Static Random- Access Memory	Biswajit Ray The University of Alabama in Huntsville	Sample Irradiation Using Ohio State University Research Reactor at the Ohio State University
Characterization of Manganese-Nickel Rich Precipitates and Their Interaction with Dislocations in Irradiated Reactor Pressure Vessel Steels	Brandon Bohanon University of Florida	Sample Preparation and Shipping Using Irradiated Materials Examination and Testing Facility at Oak Ridge National Laboratory; Post-Irradiation Examination Using Nuclear Fuels and Materials Characterization Facility at University of Florida

Project Title	PI Organization	NSUF Facilities
<i>In situ</i> Irradiation of Spent Nuclear Fuels	Cameron Howard Idaho National Laboratory	Post-Irradiation Examination Using Intermediate Voltage Electron Microscopy—Tandem Facility at Argonne National Laboratory; Sample Preparation and Shipping Using Irradiated Materials Characterization Laboratory at Idaho National Laboratory
Time-Resolved Neutron Damage Characterization Using <i>In Situ</i> Positron Annihilation Spectroscopy	Connor Harper Idaho State University	Sample Irradiation Using Ohio State University Research Reactor at the Ohio State University
Swelling Resistance of Additively Manufactured Grade 91 Steel Produced with Integrated Thermal Processing	Daniel Codd KVA Stainless	Sample Irradiation Using Michigan Ion Beam Laboratory at University of Michigan
Quantification of Local Burnup in Irradiated U-10Zr Metallic Fuel Using Atom Probe Tomography	Daniele Salvato Idaho National Laboratory	Post-Irradiation Examination Using Irradiated Materials Characterization Laboratory at Idaho National Laboratory
<i>In situ</i> High Temperature Micro-Tensile Testing of Reactor Irradiated HT9 Cladding	Fidelma Di Lemma Idaho National Laboratory	Post-Irradiation Examination Using Irradiated Materials Characterization Laboratory at Idaho National Laboratory
Understanding the Role of Nanostructuring in Enhancing Phase Stability of 304 Austenitic Steel During Irradiation via <i>In Situ</i> Ion Irradiation in Transmission Electron Microscope	Haiming Wen Missouri University of Science and Technology	Post-Irradiation Examination Using Intermediate Voltage Electron Microscopy—Tandem Facility at Argonne National Laboratory
Understanding Fundamental Effect of Grain Structure on Microstructure Evolution in HT9 via <i>In Situ</i> Irradiation and TEM	Hyosim Kim Los Alamos National Laboratory	Post-Irradiation Examination Using Intermediate Voltage Electron Microscopy—Tandem Facility at Argonne National Laboratory
Probing the Chemical Composition and Charge Status of Secondary Phases and Precipitates in High Burnup Metallic Fuel Using Nano-SIMS and TEM-EELS	Indrajit Charit University of Idaho	Post-Irradiation Examination Using Irradiated Materials Characterization Laboratory at Idaho National Laboratory
Characterization of Fluff Region in an EBR-II Metallic Fuel Pin	Jake Fay Rensselaer Polytechnic Institute	Post-Irradiation Examination Using Hot Fuel Examination Facility, Irradiated Materials Characterization Laboratory at Idaho National Laboratory

Project Title	PI Organization	NSUF Facilities
Preliminary Testing of Additively Manufactured UO ₂	Lin Shao Texas A&M University	Post-Irradiation Examination Using Irradiated Materials Characterization Laboratory at Idaho National Laboratory; Sample Preparation and Shipping Using Accelerator Laboratory at Texas A&M University
In Situ Irradiation and RF Characterization of Langasite-Based Surface Acoustic Wave Sensors for Advanced Nuclear Reactor Applications	Mauricio Pereira da Cunha University of Maine	Sample Irradiation Using Ohio State University Research Reactor at the Ohio State University
Determining Mechanical Properties of the Phases Formed of Irradiated U-19Pu-10Zr	Mitchell Mika University of Florida	Post-Irradiation Examination Using Irradiated Materials Characterization Laboratory at Idaho National Laboratory
Probing Interface Metastability as a Response to Radiation in Compositionally Complex Alloys	Mitra Taheri John Hopkins University	Post-Irradiation Examination Using Intermediate Voltage Electron Microscopy—Tandem Facility at Argonne National Laboratory
lon Irradiation and Post Characterization on Additively Manufactured High Entropy Alloys for Nuclear Applications	Mohan Sai Kiran Kumar Yadav Nartu Pacific Northwest National Laboratory	Post-Irradiation Examination Using Materials Science and Technology Laboratory, Radiochemical Processing Laboratory at Pacific Northwest National Laboratory; Sample Preparation and Shipping Using Materials Science and Technology Laboratory, Radiochemical Processing Laboratory at Pacific Northwest National Laboratory; Sample Irradiation Using University of Wisconsin Ion Beam Laboratory at University of Wisconsin
Atom Probe Tomography and Transmission Electron Microscopy of Neutron-Irradiated Nanocrystalline Compositionally Complex Alloys	Nathan Curtis University of Wisconsin- Madison	Post-Irradiation Examination Using Hot Fuel Examination Facility, Irradiated Materials Characterization Laboratory at Idaho National Laboratory
Defect Evolution in Irradiated Superior Heat Conductors	Shuxiang Zhou Idaho National Laboratory	Post-Irradiation Examination Using Microscopy and Characterization Suite at Center for Advanced Energy Studies; Sample Preparation and Shipping Using ATR Critical Facility, Irradiated Materials Characterization Laboratory at Idaho National Laboratory; Sample Irradiation Using Michigan Ion Beam Laboratory at University of Michigan
Microstructural Defect Induced Thermal Conductivity Reduction in Uranium Nitride and Thorium Nitride	Zilong Hua Idaho National Laboratory	Post-Irradiation Examination Using Irradiated Materials Characterization Laboratory at Idaho National Laboratory; Sample Irradiation Using Accelerator Laboratory at Texas A&M University



REPORTS

hrough its Rapid Turnaround Experiment and Consolidated Innovative Nuclear Research calls, the NSUF grants access to its facilities for researchers to conduct their studies to further the understanding of the effects of irradiation on nuclear fuels and materials.

The following reports resulted from these NSUF projects.

Technical Reports

Irradiation Influence on Alloys Fabricated by Powder Metallurgy and Hot Isostatic Pressing for Nuclear Applications

X-ray Diffraction Tomography Analysis of SiC Composite Tubes Neutron-Irradiated with a Radial High-Heat Flux

Short Communications

In Situ TEM Studies on Thermodynamic Stability and Microstructural Evolution of Zirconium Hydrides in Irradiation and Thermal Environments

Irradiation Behavior of Nanostructured Ferritic/Martensitic Grade 91 Steel at High Dose

Micromechanical Testing of LWR-Irradiated Harvested Reactor Internals

Irradiation Effects on Microstructure and Mechanical Properties in a Laser Welded ODS Alloy

Examining Microstructures and Mechanical Properties of Neutron and Ion Irradiated T91, HT9 and 800H Alloys

Neutron Irradiation Effects on the Tensile Properties of Wire Arc Additive Manufactured Grade 91 Steel

Hydrogen-Retention of Yttrium Hydride Under High-temperature Proton Irradiation

TECHNICAL REPORTS

Irradiation Influence on Alloys Fabricated by Powder Metallurgy and Hot Isostatic Pressing for Nuclear Applications

Janelle P. Wharry - jwharry@purdue.edu



he objective of this study is to provide a direct, side-byside comparison between powder metallurgy with hot isostatic pressing (PM-HIP) and conventional (i.e., cast or forged) nuclear structural alloys under neutron irradiation. The pressing need to deploy advanced nuclear reactors to combat climate change requires qualification of new fuels and material. Among advancedmanufacturing processes, PM-HIP is nearest to becoming qualified for nuclear applications. This project conducted a systematic study of five common nuclear structural alloys fabricated via PM-HIP: 316L stainless steel, Grade 91 ferritic steel, SA508 low-alloy reactor pressure-vessel (RPV) steel, and Ni-based Alloys 625 and 690. All materials were irradiated side-by-side with their cast or forged counterpart in the Advanced Test Reactor to target doses of 1 and 3 dpa and target temperatures of 300°C and 400°C. Following neutron irradiation, the specimens underwent uniaxial tensile testing, nanoindentation, transmission electron microscopy, and atom probe tomography. This report summarizes these results

for all five alloys and interprets the microstructure-mechanical property relationships. The results generally point toward comparatively favorable performance of PM-HIP alloys measured against their cast or forged counterparts under irradiation. This project provides data that can be used to motivate qualification of PM-HIP fabrication for nuclear structural components. Specimens are available within the Nuclear Fuels and Materials Library, where researchers worldwide can further investigate the unique behaviors and phenomena reported and discussed herein.

Introduction

Among advanced-manufacturing technologies, PM-HIP is closest to becoming fully qualified for nuclear applications [1]. The nuclear industry seeks to replace traditional castings or forgings with PM-HIP manufacturing for lightwater reactor (LWR) [1,2] and small modular reactor (SMR) [1] internals, pressure vessels [3], and secondaryside components. PM-HIP offers many advantages over conventional alloy fabrication, including an equiaxed, fine-grained structure

[4,5], chemical homogeneity [6–10], exceptional mechanical properties [3,11–17] especially at high temperatures [18,19], fewer defects [1,2], and near-net-shaped fabrication, which reduces reliance on welding and machining [20–22]. PM-HIP-manufactured ferritic and austenitic steels and Ni-based alloys are already qualified for non-nuclear applications, alongside castings and forgings, in the ASME Boiler and Pressure Vessel Code (BPVC), Section II. More recently, the PM-HIP form of austenitic stainless steel 316L has been qualified for non-irradiationfacing nuclear applications through ASME BPVC, Section III.

Previously, little was known about the irradiation behavior of PM-HIP alloys in comparison to their conventionally fabricated counterparts. Before PM-HIP products are widely deployed as irradiation-facing components within nuclear systems, this irradiation performance must be understood. Systematic and comprehensive neutron irradiation and post-irradiation examination (PIE) campaigns are the established

This neutron irradiation and PIE campaign has demonstrated favorable irradiation performance of PM-HIP structural alloys, providing data that can support their nuclear code qualification.

norms for obtaining irradiation effects and performance data under service-relevant conditions [23,24], which can subsequently be used toward materials qualification. Because neutron irradiation and PIE campaigns can often span a decade and cost millions of dollars, qualification of new materials is a longstanding bottleneck for the nuclear power industry. This project conducted a neutron irradiation and PIE campaign to directly compare PM-HIP to cast or forged versions of six nuclear structural alloys. Results from this work can expand PM-HIP qualification for irradiation-facing components and for additional alloys.

Project Hypothesis

The objective of this project is to assess the viability of using alloys manufactured by PM-HIP for nuclearreactor structural components, to enhance their quality, weldability, and inspectability. Previously, little was known about the irradiation response of PM-HIP alloys, and even more critically, existing data did not elucidate the differences in irradiation response between PM-HIP and conventional alloys. This project seeks to understand these irradiation effects through a systematic neutron-irradiation campaign and post-irradiation microstructural and mechanical assessments.

Experimental or Technical Approach

Materials:

Six common nuclear structural alloys are included in the irradiation campaign, each fabricated by PM-HIP and by either forging or casting. The alloys were SA508, Grade 3, Class 1 low-alloy RPV steel, Ni-based Alloys 625 and 690, Grade 91 ferritic steel, and austenitic stainless steels 316L and 304L. The alloys were compliant with ASME BPVC compositional specifications and were all provided by the Electric Power Research Institute. For all alloys, HIP was conducted at a pressure of 15 ksi for 4 hours: the HIP temperature was 1149°C for the two Ni-based alloys, and 1121°C for all other alloys. The heat treatments for the HIP and cast or forged materials followed standard heat-treatment procedures for the specific alloys. The two Nibased alloys and the two austenitic stainless steels were solution cycled, then water quenched; the Grade 91 was normalized and tempered; and the SA508 was solutioncycled, quenched, normalized, and tempered. The specimen geometries were ASTM E8 round tensile bars for mechanical-property evaluation, transmission electron microscopy (TEM) discs (i.e., coupons) for microstructure characterization and nanoindentation, and precracked miniature compact-tension (CT) specimens for fracture-toughness testing. A more comprehensive description of the alloy compositions, fabrications, and heat treatment

details, as well as specimen machining methods, are described in ref. [25].

Neutron Irradiation:

For this project, the Advanced Test Reactor (ATR) at Idaho National Laboratory (INL), was selected for its high thermal-neutron flux (relative to fast flux) and lowertemperature capabilities, both of which are more representative of the LWR environments in which the studied alloys are intended to operate. Additionally, ATR offers relatively large test volumes, able to accommodate specimen geometries such as ASTM E8 standardized tensile bars for material qualification efforts. Specimens were irradiated to target doses of ~1 and 3 dpa at target temperatures of ~300°C and 400°C.

Uniaxial Tensile Testing and Fractography:

Uniaxial tensile testing of radioactive specimens was conducted using a 13M Instron load cell in the hot cells at the Hot Fuel Examination Facility (HFEF) at INL. Testing was conducted at ambient temperature in an argon environment following the ASTM E8 standard for threadedgrip specimens. The load capacity of the cell was 50 kN, and loading rate range was 0.001–500 mm/min. In the present experiments, a strain rate of $8.78 \times 10^{-3} \text{ s}^{-1} (0.279 \text{ mm/min})$ crosshead speed) was used through 10% strain, after which the strain rate increased to 3.15×10^{-2} s⁻¹ (1.0

mm/min crosshead speed) until failure. Time, load, and displacement were recorded throughout the test and have been archived in [26]. After tensile testing, fracture surfaces were cut from the broken tensile halves using a diamond wafering blade. This enabled the fracture surfaces to be oriented face-up in a scanning electron microscope (SEM) for fractography. A Lyra3 Tescan SEM at the Electron Microscopy Laboratory (EML) at INL was used for fracture-surface characterization. Fractographs are also archived in [26].

Nanoindentation:

A nanoindentation hardness measurement was conducted using the Hysitron TI-950 Tribolndenter at the Microscopy and Characterization Suite (MaCS), Center for Advanced Energy Studies (CAES). Nanoindentation is used to rapidly evaluate hardness and elastic modulus, especially in irradiation campaigns that cannot accommodate ASTM standard-sized tensile bars, or for volume-limited specimens [27]. The TI-950 can be operated with a Berkovich tip in depth-controlled or load-controlled mode, with a maximum load of 2.2 N. In the present work, nanoindentation was conducted in depth-controlled mode to a maximum depth of 3500 nm at a strain rate of 0.2 s⁻¹. The displacement and load were recorded continuously as a function of time, from which the

nanoindentation hardness was calculated using the Oliver-Pharr method [28].

Transmission Electron Microscopy:

We conducted TEM using the FEI (now Thermo Fisher) Tecnai TF30-FEG STwin TEM at MaCS, CAES. The instrument is equipped with energydispersive x-ray spectroscopy (EDS), electron energy-loss spectroscopy (EELS), energy-filtered TEM (EFTEM), scanning TEM (STEM), and TopSpin. The instrument has been used across numerous NSUF projects to characterize irradiation-induced defects, including dislocation loops, using techniques including twobeam condition (rel-rod) imaging or down-zone STEM [29], voids or bubbles using the throughfocus technique, phase evolution using diffraction and EDS, and nanoclustering and radiationinduced segregation using EDS line and area mapping. To evaluate the performance of PM-HIP alloys, the TEM characterization focused on precipitate, dislocation-loop, and void evolution under irradiation. In this work, the TEM was operated in STEM mode at 200 kV. STEM highangle annular dark field (HAADF) imaging was used to observe the precipitate number density and distribution, with high-resolution STEM to observe the precipitate structures. Bright-field down-zone STEM imaging was used to observe dislocation loops, following a

technique described in [29]. Voids (when present) were imaged using through-focusing.

Atom Probe Tomography:

We conducted 3D atomic-scale chemical characterization using the CAMECA Local Electrode Atom Probe (LEAP) 4000X HR at MaCS, CAES dedicated for radioactive specimens. Atom probe tomography (APT) uses the principle of field evaporation on a ~10-100-nm-diameter needle specimen; the evaporated species from the needle are collected in a time-of-flight mass spectrometer, enabling atom-by-atom positionsensitive 3D reconstruction of the needles. The LEAP 4000X HR at CAES is capable of laser or voltage pulsing with 250-kHz laser or 200-kHz voltage-pulse generator. Metallic specimens can often be analyzed using voltage pulsing for high mass resolution; however, specimens having limited conductivity must be analyzed using laser pulsing, which may limit mass resolution [30]. In the current work, specimens were tested in laser-pulse mode with 60pJ laser energy, a 200-kHz pulse rate, and specimen base temperature ~50 K. APT raw data files were reconstructed using the CAMECA proprietary AP Suite software, with cluster analysis conducted following established procedures [31–35].

Results

GRADE 91: The Grade 91 ferritic steel results are summarized in Figure 1. Grade 91 exhibited conventional irradiation hardening and loss of ductility, with the PM-HIP version typically exhibiting less hardening and greater retention of ductility than the cast version. The more interesting mechanical behavior that emerges is the presence of a load drop immediately after plastic yielding, often called the yield-point phenomenon. This load drop occurs in both the PM-HIP and cast specimens at 1 dpa, although it is more pronounced in the PM-HIP specimen.

Considering the microstructure can explain the emergence of this load drop. Both the PM-HIP and cast materials exhibit a high initial dislocation density before irradiation. But dislocation recovery occurs extensively during irradiation, with the irradiated microstructures exhibiting a relatively low dislocation density. At the same time, irradiation also induces the nucleation of dislocation loops. When dislocation recovery and loop nucleation are occurring simultaneously, the loops may be pinning the remaining dislocation lines. Consequently, the irradiated microstructures—especially at 1 dpa—exhibit a heterogeneous dislocation-loop distribution, in which loops tend to cluster along dislocation lines. This heterogeneous loop distribution persists through 3 dpa, with loops further nucleating

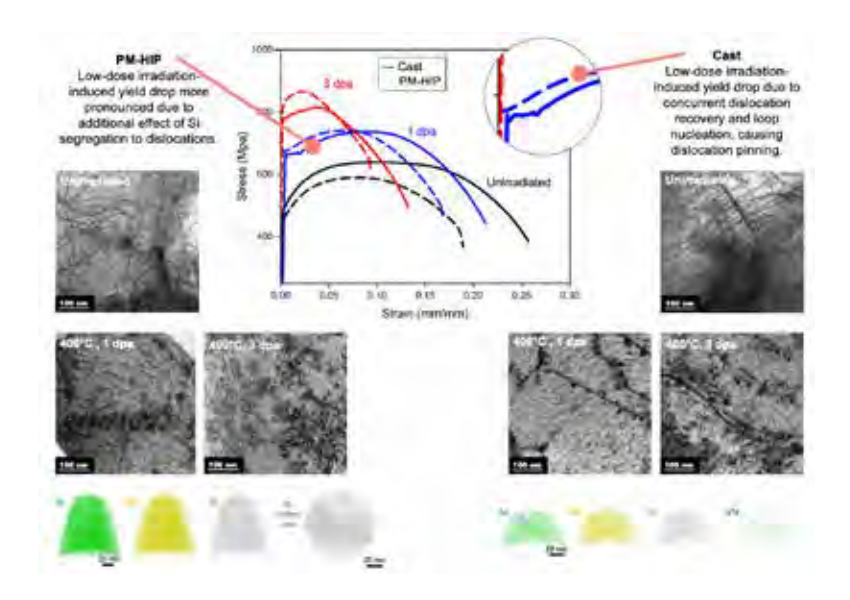


Figure 1: Summary of neutron-irradiated mechanical property and microstructure evolution in PM-HIP and cast Grade 91 ferritic steel at doses of \sim 1 and \sim 3 dpa at \sim 400°C.

along dislocation lines, essentially forming subgrain-type structures. The pinning of dislocation lines on loops can explain the load-drop phenomenon; that is, the loops act as strong obstacles to the dislocation motion, and after they unpin at yielding, an overall stress relief presents itself as a load drop. Quantitatively, the PM-HIP and cast dislocation microstructures are statistically similar, suggesting little-to-no difference in irradiated microstructure evolution based on processing method.

The PM-HIP's exhibiting a more pronounced load drop than the cast material may be associated with the APT results. APT results show that fine Ni-Mn-Si nanoclusters are present in both the cast and PM-HIP specimens. Nanoclusters in the cast specimen also contain vanadium nitride (VN) and vanadiaum

carbide (VC) molecules, while those in the PM-HIP specimen do not. Quantitatively, the PM-HIP and cast nanoclusters are statistically identical, though the PM-HIP has slightly smaller nanocluster diameters and volume fractions than the cast specimen. However, the more notable difference is that the PM-HIP specimen appears to exhibit Suzuki-like segregation of the clustering species to dislocation features, particularly Si. This chemical segregation provides an additional barrier for dislocation motion, which could result in the more-pronounced stress relief (i.e., load drop) after the dislocations begin to glide.

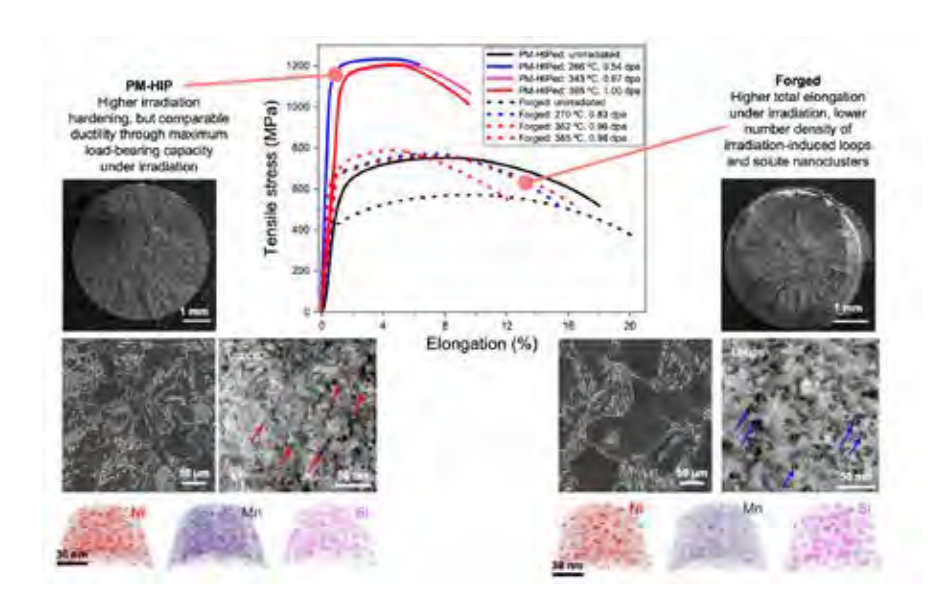


Figure 2: Summary of neutron-irradiated mechanical property and microstructure evolution in PM-HIP and forged SA508 low-alloy RPV steel at doses of \sim 1 dpa at \sim 300°C and \sim 400°C.

SA508: The SA508 RPV steel results are summarized in Figure 2. The mechanical behavior of the PM-HIP material is striking, even before irradiation. The unirradiated PM-HIP specimen exhibits ~120 MPa higher yield strength and ~180 MPa higher ultimate tensile strength (UTS) without significant loss of uniform elongation (UE) and total elongation (TE), as compared to the reference forged material. Mechanical behaviors between PM-HIP and forged materials deviate even more after irradiation, with both materials exhibiting yield strength and UTS increases leading to irradiation hardening, with a reduction in ductility. The PM-HIP specimens show significantly higher irradiation hardening than their forged counterparts. However, the effects of irradiation on ductility and toughness do not necessarily

follow irradiation-hardening trends. Although the TE of the irradiated PM-HIP specimens is almost half that of the irradiated forged specimens, the post-irradiation UE after irradiation is relatively consistent across both fabrication methods. Thus, although TE to fracture is severely compromised in the irradiated PM-HIP material compared to the forging, both processing methods exhibit comparable ductility through their respective maximum load-bearing capacities. Fracture surfaces of the PM-HIP material exhibit a relatively flat surface, free of dimples, characteristic of brittle fracture. Meanwhile, the forged material exhibits a relatively flat region in the center of the tensile bar with cup-cone like features around the periphery of the bar with some dimpling, suggesting a combination of brittle and ductile fracture modes.

Fractography corroborates the tensile testing results.

TEM characterization of dislocation loops in the irradiated PM-HIP and forged SA508 provide some insight into the relative differences in their mechanical behaviors. Loop sizes for PM-HIP SA508 are roughly half that of forged SA508, but the number density of loops in PM-HIP SA508 is ~8 times that in forged SA508 under the same irradiation conditions. These loop number densities suggest greater susceptibility to loop nucleation in the PM-HIP than in the forged material. Similarly, APT reconstructions show evidence of Mn-Ni-Si-rich precipitate (MNSP) nucleation in both the PM-HIP and forged materials. Like loops, the average nanoprecipitate sizes are statistically identical in both alloys, but they occur at a higher number density in the PM-HIP than in the forged material.

The greater dislocation-loop density in the PM-HIP alloy may be due to its chemical composition. In RPV steels at doses above ~0.1 dpa, irradiation drives Mn-Ni-Si (MNS) or Mn-Ni-Si-P (MNSP) nanoclusters to agglomerate on point defect clusters [36-38]. This muddles the distinction between nanoclusters and defect clusters, the latter of which grow into dislocation loops at higher fluences [38-42]. Once these loops become large enough to be resolved in TEM, they are often decorated by Mn and Ni (and Cu, if present in the bulk material) [43,44].

This underscores the importance of Mn and Ni in stabilizing the loop and nanoprecipitate population. The higher bulk concentration of Mn and Ni in the PM-HIP alloy (1.39 wt% and 0.79 wt%, respectively) than in the forged alloy (0.46 wt% Mn and 0.50 wt% Ni) can explain the higher loopnumber densities in the PM-HIP alloy. This finding suggests that irradiation susceptibility of RPV steels may be more strongly influenced by bulkalloy chemistry than processing method.

ALLOY 625 & 690: The results from Ni-based Alloy 625 and Alloy 690 are summarized in Figure 3. Both alloys exhibit increases in yield strength and UTS during irradiation, and decreases in elongation, all characteristic of classic irradiation hardening and embrittlement. The extent of hardening and embrittlement tends to increase with irradiation dose from ~1 to ~3 dpa. There is no significant or notable difference in the mechanical response of the PM-HIP versions of the alloys, compared to that of the forged versions.

The microstructure evolution under irradiation can reasonably well reasonably account for mechanical behaviors. Conventional irradiation-induced loops and voids are found in both the PM-HIP and forged versions of both Alloy 625 and Alloy 690. The quantitative loop and void sizes and number densities between both processing methods are statistically similar, which explains the similar mechanical responses.

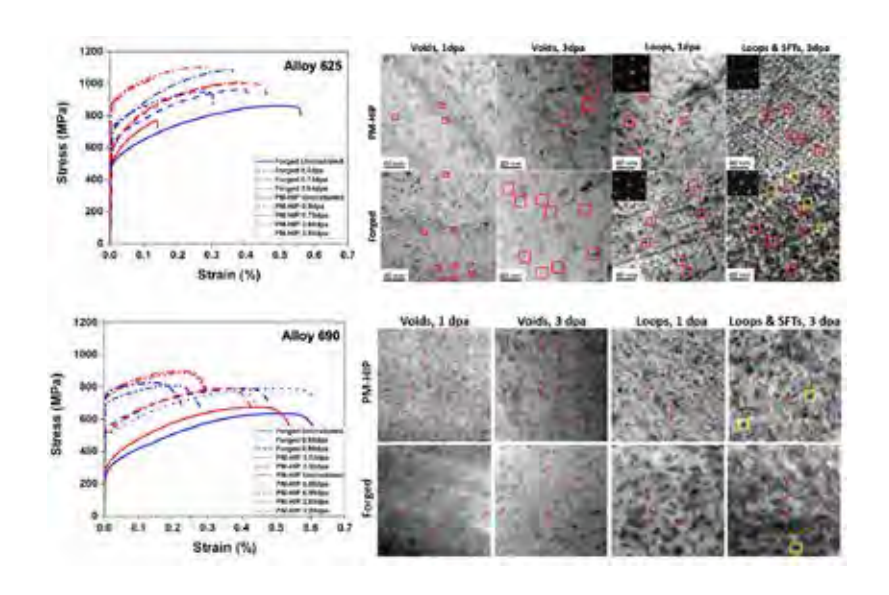


Figure 3: Summary of neutron-irradiated mechanical property and microstructure evolution in PM-HIP and forged Alloy 625 and Alloy 690 Ni-based alloys at doses of \sim 1 and \sim 3 dpa at \sim 400°C.

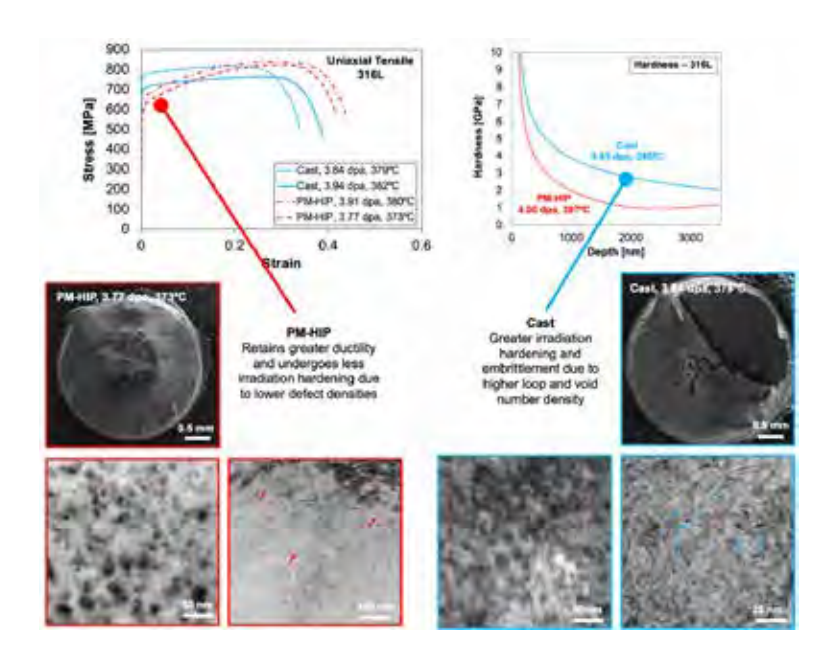


Figure 4: Summary of neutron-irradiated mechanical property and microstructure evolution in PM-HIP and cast 316L stainless steel at doses of \sim 4 dpa at \sim 400°C.

With increasing irradiation dose, from ~1 to ~3 dpa, the void and loop sizes increase while the number densities decrease in all specimens, as is indicative of typical coarsening behavior. At ~3 dpa, triangular-shaped features characteristic of stacking-fault tetrahedra (SFTs) are observed in both the PM-HIP and forged versions of Alloy 690, and in the forged version of Alloy 625. SFTs are strong obstacles for dislocation motion, explaining the higher hardening and embrittlement at these doses.

316L SS: Results from irradiated 316L SS are summarized in Figure 4. After irradiation, the PM-HIP specimens exhibit ~10–15% greater ductility than the cast specimens. Although the irradiated PM-HIP specimens have a lower yield strength than the cast specimens, the PM-HIP specimens have a greater strain-hardening capacity, resulting in a higher ultimate tensile stress (UTS) than the cast specimens. The lower ductility of the cast specimen is evident from fractography, which shows a relative flat, dimple-free fracture surface with possible tearing-type behavior in the cast specimen; by contrast, the PM-HIP specimen exhibits a classic ductile cup-conetype fracture surface that is highly dimpled.

Nanoindentation load-displacement curves show that a higher load

is required to reach the same indent depth in the cast specimen than as in the PM-HIP specimen; correspondingly, the cast material has a higher hardness by ~1.5 GPa. With relatively negligible differences in the actual irradiation dose and temperature between the cast and PM-HIP specimens, the hardness difference is, thus, likely a true hardness difference that can be ascribed to the material microstructure. This behavior is consistent with the lower yield strength and higher strain hardenability of PM-HIP 316L observed in uniaxial tensile testing.

In the unirradiated states, the PM-HIP exhibits higher yield strength than the forged specimen [17], explained by the Hall-Petch relationship and the finer-grained structure of the PM-HIP material. However, under irradiation, a finer grain structure provides a high sink density that facilitates recombination of irradiationinduced defects [45-49]. Hence, the finer grain structure may make the PM-HIP 316L more irradiationtolerant than forged 316L, thus accumulating a lesser extent of irradiation hardening. Indeed irradiation-induced dislocation loops and voids are more prevalent in the cast than in the PM-HIP material. These features explain the greater irradiation hardening and embrittlement in the cast specimens than in the PM-HIP specimens.

Discussion

Across all five alloys studied, there are no significant differences in the irradiated microstructure evolution when comparing the PM-HIP and the cast or forged counterpart. Differences are most likely ascribed to bulk concentrations and grain-size differences, rather than to any inherent characteristic of the fabrication process. In all cases but SA508, the PM-HIP tends to perform favorably compared to the cast or forged material on a quantitative, microstructural basis. These microstructural behaviors translate to mechanical properties, with the PM-HIP materials typically performing comparably or better than the cast or forged material. Most of the mechanical properties can be ascribed to the observed microstructure evolution through the Orowan-dispersed-barrier hardening model.

The favorable overall irradiation performance of PM-HIP alloys in comparison to their conventionally manufactured counterparts provides the impetus for qualification and deployment of PM-HIP as a fabrication method for heavy components in both current and future nuclear power plants. The use of PM-HIP manufacturing can improve the economics of heavy-component fabrication and reinvigorate domestic manufacturing, enabling the Department of Energy, Office of Nuclear Energy, to meet its goals of delivering reliable, cost-effective new reactors and extending the life of current reactors.

Conclusion

This project generated irradiation-performance data on PM-HIP, as compared to cast or forged nuclear-structural materials, through a comprehensive irradiation and post-irradiation examination campaign. The overall irradiation campaign enabled a systematic comparison of mechanical and microstructural evolution between the PM-HIP and conventionally fabricated variants. Results generally show favorable irradiation performance of PM-HIP Grade 91, 316L stainless steel, and Ni-based Alloy 625 and 690, in comparison to their cast or forged versions. However, PM-HIP-manufactured low-alloy RPV steel SA508 exhibited somewhat poorer irradiation performance; also, some of its features, such as irradiated uniform elongation, are favorable.

Future code-qualification efforts for the respective PM-HIP alloys may leverage these data as evidence of the irradiation resilience of PM-HIP materials relative to the already-qualified methods of casting or forging. This NSUF project may also serve as a model for future irradiation and PIE experiments seeking to generate nuclear-code qualification data for new fuels and materials, advanced manufacturing methods, or advanced welding and joining technologies. The breadth of NSUF capabilities leveraged herein can also provide a template for designing future NSUF-supported programs to evaluate structure-property relationships in irradiated materials and fuels.

Future Activities

All specimens described in this work are available in the NSUF Nuclear Fuels and Materials Library, through which they are openly and competitively available to the community for follow-on research. Tremendous opportunities exist for fundamental follow-on studies to mechanistically investigate the many interesting phenomena observed herein. For example, these results prompt fundamental questions such as:

- What exactly is the cause of the load drop in Grade 91? Why has its
 heterogeneous loop-microstructure evolution not been observed or
 reported at higher doses typically studied in Grade 91 and similar ferritic/
 martensitic steels?
- Can we tailor the compositions of the SA508 PM-HIP alloy to be closer to that of the forged material, thus eliminating composition as a variable in comparing fundamental irradiation behaviors?
- What is the role of grain-size and phase-fraction differences in controlling the irradiation tolerance of SA508 and 316L stainless steel?
- Why do SFTs form more readily in forgings than in PM-HIP Ni-based alloys? Why are SFTs not observed in 316L?

More practically, this work shows the need for fracture toughness testing using Charpy or compact-tension specimens (which were irradiated, but not tested, during this project). These fracture data are the remaining piece necessary to support a code case for qualifying PM-HIP alloys for nuclear applications.

References

- [1.] D. W. Gandy, C. Stover, K. Bridger, and S. Lawler, Materials Research Proceedings (Hot Isostatic Pressing: HIP'17) 10, 224 (2019).
- [2.] D. W. Gandy, J. Shingledecker, and J. Siefert, Advanced Materials & Processes 170, 1 (2012).
- [3.] A. Morrison, J. Sulley, C.
 Carpenter, B. Borradaile,
 G. Jones, and T. Warner,
 The Proceedings of the
 International Conference on
 Nuclear Engineering (ICONE)
 27, 1021 (2019).
- [4.] C. Clement, Y. Zhao, P. Warren, X. Liu, S. Xue, D. W. Gandy, and J. P. Wharry, Journal of Nuclear Materials 558, 153390 (2022).
- [5.] C. Clement, S. Panuganti, P. H. Warren, Y. Zhao, Y. Lu, K. Wheeler, D. Frazer, D. P. Guillen, D. W. Gandy, and J. P. Wharry, Materials Science and Engineering: A 857, 144058 (2022).
- [6.] D. W. Gandy, J. Siefert, R. Smith, P. Anderson, L. Lherbier, D. Novotnak, S. Babu, and D. Sandusky, in World PM2016 (2016).
- [7.] R. Ahmed, A. Ashraf, M. Elameen,N. H. Faisal, A. M. El-Sherik,Y. O. Elakwah, and M. F. A.Goosen, Wear 312, 70 (2014).

- [8.] H. Yu, R. Ahmed, H. Villiers Lovelock de, and H. Davies, Journal of Tribology (Transactions of the ASME) 131, 011601.1 (2009).
- [9.] R. Ahmed, H. L. De Villiers Lovelock, S. Davies, and N. H. Faisal, Tribol Int 57, 8 (2013).
- [10.] A. V. Shulga, Journal of Nuclear Materials 434, 133 (2013).
- [11.] H. Atkinson and S. Davies, Metallurgical and Materials Transactions A 31A, 2981 (2000).
- [12.] G. A. Rao, M. Kumar, M. Srinivas, and D. S. Sarma, Materials Science and Engineering A 355, 114 (2003).
- [13.] Metals and Ceramics Information Center Report No. MCIC-77-34 (November 1977) (Columbus, Ohio, 1977).
- [14.] A. V. Shulga, in Euro PM 2012 -Hot Isostatic Pressing 3 (2012), pp. 1–6.
- [15.] A. V. Shulga, Euro PM 2014 Congress and Exhibition, Proceedings 1 (2014).
- [16.] T. S. Barros, P. H. R. Pecly, J. M. Pardal, A. C. Gonzaga, and S. S. M. Tavares, J Mater Eng Perform (2022).
- [17.] D. P. Guillen, D. C. Pagan, E. M. Getto, and J. P. Wharry, Materials Science & Engineering A 738, 380 (2018).

- [18.] A. L. Bullens, E. Bautista, E. H. Jaye, N. L. Vas, N. B. Cain, K. Mao, D. W. Gandy, and J. P. Wharry, JOM 70, 2218 (2018).
- [19.] E. M. Getto, B. Tobie, E. Bautista, A. L. Bullens, Z. T. Kroll, M. J. Pavel, K. S. Mao, D. W. Gandy, and J. P. Wharry, JOM 71, 2837 (2019).
- [20.] K. S. Mao, Y. Wu, C. Sun, E. Perez, and J. P. Wharry, Materialia (Oxf) 174 (2018).
- [21.] K. Mao, H. Wang, Y. Wu, V. Tomar, and J. P. Wharry, Materials Science and Engineering A 721, 234 (2018).
- [22.] K. S. Mao, A. J. French, X. Liu, Y. Wu, L. A. Giannuzzi, C. Sun, M. Dubey, P. D. Freyer, J. K. Tatman, F. A. Garner, L. Shao, and J. P. Wharry, Mater Des 206, 109764 (2021).
- [23.] D. C. Crawford, D. L. Porter, S. L. Hayes, M. K. Meyer, D. A. Petti, and K. Pasamehmetoglu, Journal of Nuclear Materials 371, 232 (2007).
- [24.] D. Petti, J. Maki, J. Hunn, P. Pappano, C. Barnes, J. Saurwein, S. Nagley, J. Kendall, and R. Hobbins, JOM 62, 62 (2010).
- [25.] D. P. Guillen, J. P. Wharry, G. Housley, C. D. Hale, J. Brookman, and D. W. Gandy, Nuclear Engineering and Design 402, 112114 (2023).

- [26.] J. P. Wharry, C. D. Clement, Y. Zhao, K. Baird, D. Frazer, J. Burns, Y. Lu, Y. Q. Wu, C. Knight, D. P. Guillen, and D. W. Gandy, Data Brief 48, 109092 (2023).
- [27.] T. Chen, L. He, M. H. Cullison, C. Hay, J. Burns, Y. Wu, and L. Tan, Acta Mater 195, 433 (2020).
- [28.] W. C. Oliver and G. M. Pharr, J Mater Res 19, 3 (2004).
- [29.] C. M. Parish, K. G. Field, A. G. Certain, and J. P. Wharry, J Mater Res 30, 1275 (2015).
- [30.] A. Sen, M. Bachhav, F. Vurpillot, J. M. Mann, P. K. Morgan, T. A. Prusnick, and J. P. Wharry, Ultramicroscopy 220, 113167 (2021).
- [31.] D. Vaumousse, A. Cerezo, and P. J. Warren, Ultramicroscopy 95, 215 (2003).
- [32.] C. A. Williams, D. Haley, E. A. Marquis, G. D. W. Smith, and M. P. Moody, Ultramicroscopy 132, 271 (2013).
- [33.] J. M. Hyde, E. A. Marquis, K. B. Wilford, and T. J. Williams, Ultramicroscopy 111, 440 (2011).
- [34.] M. J. Swenson and J. P. Wharry, Journal of Nuclear Materials 467, 97 (2015).
- [35.] M. J. Swenson and J. P. Wharry, Microscopy and Microanalysis 22, 690 (2016).

- [36.] 36. G. Bonny, D. Terentyev, A. Bakaev, E. E. Zhurkin, M. Hou, D. Van Neck, and L. Malerba, Journal of Nuclear Materials 442, 282 (2013).
- [37.] G. Bonny, D. Terentyev, E. E. Zhurkin, and L. Malerba, Journal of Nuclear Materials 452, 486 (2014).
- [38.] E. Meslin, M. Lambrecht,
 M. Hernández-Mayoral, F.
 Bergner, L. Malerba, P. Pareige,
 B. Radiguet, A. Barbu, D.
 Gómez-Briceño, A. Ulbricht,
 and A. Almazouzi, Journal
 of Nuclear Materials 406, 73
 (2010).
- [39.] J. Kočık, E. Keilová, J. Čıžek, and I. Procházka, Journal of Nuclear Materials 303, 52 (2002).
- [40.] G. Maussner, L. Scharf, R. Langer, and B. Gurovich, Nuclear Engineering and Design 193, 359 (1999).
- [41.] E. A. Kuleshova, B. A. Gurovich, Ya. I. Shtrombakh, D. Yu. Erak, and O. V. Lavrenchuk, Journal of Nuclear Materials 300, 127 (2002).
- [42.] B. A. Gurovich, E. A. Kuleshova, Ya. I. Shtrombakh, D. Yu. Erak, A. A. Chernobaeva, and O. O. Zabusov, Journal of Nuclear Materials 389, 490 (2009).
- [43.] K. Fujii, K. Fukuya, N. Nakata, K. Hono, Y. Nagai, and M. Hasegawa, Journal of Nuclear

- Materials 340, 247 (2005).
- [44.] T. Hamaoka, Y. Satoh, and H. Matsui, Journal of Nuclear Materials 399, 26 (2010).
- [45.] C. Du, S. Jin, Y. Fang, J. Li, S. Hu, T. Yang, Y. Zhang, J. Huang, G. Sha, Y. Wang, Z. Shang, X. Zhang, B. Sun, S. Xin, and T. Shen, Nat Commun 9, 5389 (2018).
- [46.] X. Zhang, K. Hattar, Y. Chen, L. Shao, J. Li, C. Sun, K. Yu, N. Li, M. L. Taheri, H. Wang, J. Wang, and M. Nastasi, Prog Mater Sci 96, 217 (2018).
- [47.] P. V. Patki, Y. Q. Wu, and J. P. Wharry, Materialia (Oxf) 9, 100597 (2020).
- [48.] G. R. Odette and D. T. Hoelzer, JOM 62, 84 (2010).
- [49.] K. Y. Yu, C. Sun, Y. Chen, Y. Liu, H. Wang, M. A. Kirk, M. Li, and X. Zhang, Philosophical Magazine 93, 3547 (2013).

Publications

- [1.] W. Jiang, Y. Zhao, Y. Lu, D. Frazer, D.P. Guillen, D.W. Gandy, and J.P. Wharry. Comparison of PM-HIP to forged SA508 pressure vessel steel under high-dose neutron irradiation. Under revision at Journal of Nuclear Materials as of January 2024.
- [2.] [INVITED] J.P. Wharry, D.P.
 Guillen, C.D. Clement, S. Bin
 Habib, W. Jiang, Y. Lu, Y.Q.
 Wu, C.-H. Shiau, D. Frazer,
 B. Heidrich, C. Knight, and
 D.W. Gandy. Materials
 qualification through the
 Nuclear Science User Facilities
 (NSUF): A case study on
 irradiated PM-HIP structural
 alloys. Frontiers in Nuclear
 Engineering 2 (2023) 1306529.
 https://doi.org/10.3389/
 fnuen.2023.1306529.
- [3.] J.P. Wharry, C.D. Clement, Y. Zhao, K. Baird, D. Frazer, J. Burns, Y. Lu, Y.Q. Wu, C. Knight, D.P. Guillen, and D.W. Gandy. Mechanical testing data from neutron irradiations of PM-HIP and conventionally manufactured nuclear structural alloys. Data in Brief 48 (2023) 109092. https://doi.org/10.1016/j. dib.2023.109092.

- [4.] D.P. Guillen, J.P. Wharry, G.K.
 Housley, C.D. Hale, J.V.
 Brookman, and D.W. Gandy.
 Irradiation experiment
 design for the evaluation
 of PM-HIP alloys for nuclear
 reactors. Nuclear Engineering
 & Design 402 (2023) 112114.
 https://doi.org/10.1016/j.
 nucengdes.2022.112114.
- [5.] C.D. Clement, S.S. Panuganti, P.H. Warren, Y. Zhao, Y. Lu, K. Wheeler, D. Frazer, D.P. Guillen, D.W. Gandy, and J.P. Wharry. Comparing structure-property evolution for PM-HIP and forged Alloy 625 irradiated with neutrons to 1 dpa. Materials Science & Engineering A 857 (2022) 144058. https://doi.org/10.1016/j.msea.2022.144058.
- [6.] C.D. Clement, Y. Zhao, P.H. Warren, X. Liu, S. Xue, D.W. Gandy, and J.P. Wharry. Comparison of ion irradiation effects in PM-HIP and forged Alloy 625. Journal of Nuclear Materials 558 (2022) 153390. https://doi.org/10.1016/j.jnucmat.2021.153390.

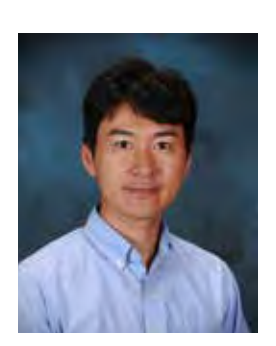
- [7.] E. Getto, B. Tobie, E. Bautista, A.L. Bullens, Z.T. Kroll, M.J. Pavel, K.S. Mao, D.W. Gandy, and J.P. Wharry. Thermal aging and Hall-Petch relationship of PM-HIP and wrought Alloy 625. JOM 71.8 (2019) 2837-2845. http://doi.org/10.1007/s11837-019-03532-6.
- [8.] D.P. Guillen, D.C. Pagan, E.M. Getto, and J.P. Wharry. *In situ* tensile study of PM-HIP and cast 316L stainless steel and Inconel 625 alloys with high energy diffraction microscopy. Materials Science and Engineering A 738 (2018) 380-388. http://doi.org/10.1016/j.msea.2018.09.083.
- [9.] E. Getto, B. Tobie, E. Bautista, A. Bullens, D.W. Gandy, and J.P. Wharry. Grain evolution in thermally aged cast and hot isostatic pressed Inconel 625. Microscopy & Microanalysis 24.S1 (2018) 666-667. http://doi.org/10.1017/S1431927618003823.
- [10.] A. Bullens, E. Bautista, E.H. Jaye, N. Vas, N.B. Cain, K. Mao, D.W. Gandy, and J.P. Wharry. Comparative thermal aging effects on PM-HIP and forged Inconel 690. JOM 70.10

- (2018) 2218-2223. http://doi.org/10.1007/s11837-018-2818-z.
- [11.] D.P. Guillen, J.P. Wharry, and D.W. Gandy. Neutron irradiation of nuclear structural materials fabricated by powder metallurgy with hot isostatic pressing. ANS Transactions 116 (2017) 392-393.

Distributed Partnership at a Glance		
NSUF Institution	Facilities and Capabilities	
Center for Advanced Energy Studies Idaho National Laboratory	Microscopy and Characterization Suite (MaCS) Advanced Test Reactor	
Collaborators		
Electric Power Research Institute	David W. Gandy (Co-Principal Investigator)	
Purdue University	Janelle P. Wharry (Principal Investigaror) Caleb D. Clement (Team Member) Saquib Bin Habib (Team Member) Sri Sowmya Panuganti (Team Member) Wen Jiang (Team Member) Yangyang Zhao(Team Member)	
United States Naval Academy	Elizabeth Getto (Collaborator)	

X-ray Diffraction Tomography Analysis of SiC Composite Tubes Neutron-Irradiated with a Radial High-Heat Flux

Takaaki Koyanagi - koyanagit@ornl.gov



he overarching project goal is to investigate lattice-strain distribution in silicon carbide composite (SiC) tubing, subject to neutron irradiation under a radial high-heat flux, which is relevant to practical light-water reactor (LWR) fuel operation. It uses XRD-CT techniques to experimentally verify modeling results for the stress state. This knowledge will aid improvement of the thermomechanical modeling capability for a SiC-based accidenttolerant fuel (ATF) cladding for LWRs. The specific project goal is to demonstrate the feasibility of the strain mapping.

Introduction

SiC-fiber-reinforced SiC matrix (SiC/ SiC) composites are of interest for ATF cladding in LWRs because of their high strength at elevated temperatures, relatively low neutron absorption, and steam-oxidation resistance. However, modeling work predicted that thermal gradients can significantly affect the stress states of SiC components during irradiation because of inversely temperaturedependent, irradiation-induced swelling. The temperature gradient is produced by the temperature difference between the fuel and water coolant. This temperaturedependent swelling is known to play a major role in the stress state of irradiated cladding in normal operational environments.

The current knowledge gap lies in experimental quantification of the irradiation-induced stress in SiC tubular materials. To experimentally evaluate such stress, this research extracted data on lattice strain in these tubes to understand the effects of temperature gradients under irradiation. The experiment used state-of-the-art synchrotron x-ray diffraction at the National Synchrotron Light Source II X-ray Powder Diffraction beamline at Brookhaven National Laboratory, part of the NSUF. Specimens were prepared at the Low Activation Materials Design and Analysis (LAMDA) Laboratory at Oak Ridge National Laboratory.

Experimental or Technical Approach

The work involved XRD-CT analysis of a section of SiC tubes as-fabricated and neutron-irradiated with a through-thickness temperature gradient. The XRD-CT analysis provided both 2D and 3D distributions of lattice strain. This nondestructive method effectively and directly evaluated residual stress in this ceramic material.

Synchrotron-based x-ray-diffraction tomography enables nondestructive evaluation of irradiated SiC-composite tube material for ATF/cladding applications.

Results

A series of XRD scans and peak analysis revealed that high-quality diffraction data can be obtained even from the irradiated SiC tube specimen—using the CT setting (Fig. 1). The XRD spectra were explained by the F-43 m crystal phase of 3C-SiC, and a small shoulder of (111) peak was attributed to stackingfault defects. Statistical analysis of the lattice parameter of the as-fabricated SiC-tube specimens showed a deviation of $\pm 0.1\%$. This relatively large deviation is likely due to the heterogeneous microstructure of the composite material (e.g., presence of processinduced residual strain) and is much larger than the lattice parameter uncertainty, as analyzed by Rietveld refinement.

Discussion

To use the XRD-CT technique for nondestructive evaluation of irradiated SiC tubes, the uncertainty of the lattice-constant evaluation should be much better than the irradiation-induced lattice expansion of \sim 0.5%. The \pm 0.1% deviation of lattice constant in the as-fabricated specimen can hinder understanding the distribution of irradiationinduced lattice expansion within the tube specimen. One potential solution is to compare XRD-CT data obtained from the same area within a SiC tube specimen before and after neutron irradiation. With this approach, the deviation of the lattice constant in the as-fabricated specimen does not affect the evaluation of irradiation-induced lattice changes.

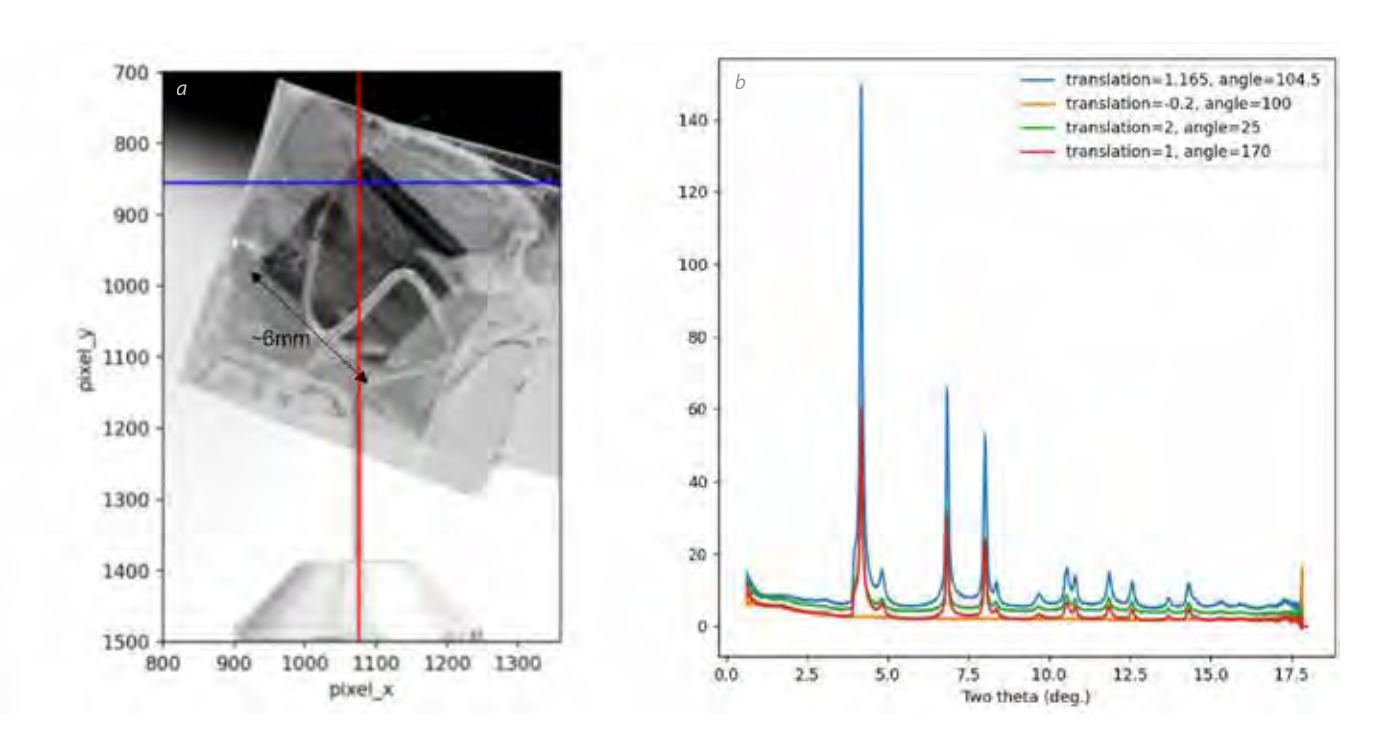


Figure 1. (a) Section of neutron-irradiated SiC composite tube used for XRD-CT experiments, and (b) XRD spectra collected with different translations (in mm) and rotation angles (in degree).

Conclusion

This research demonstrated the potential of the XRD-CT analysis technique for nondestructive evaluation of irradiated SiC tubes relevant to SiC-based ATF cladding for LWR applications. Acquisition of XRD-CT data before and after irradiation from the same specimen is key to obtaining high-quality data to investigate lattice strain within an irradiated SiC tube.

Future Activities

Further work will be conducted to better understand deformation mechanisms under high doses, via atomistic modeling and simulation.

Distributed Partnership at a Glance		
NSUF Institution	Facilities and Capabilities	
Brookhaven National Laboratory	National Synchrotron Light Source II	
Oak Ridge National Laboratory	Low Activation Materials Design and Analysis Laboratory (LAMDA)	
Collaborators		
Oak Ridge National Laboratory	Takaaki Koyanagi (Principal Investigator) Yutai Katoh (Co-Principal Investigator)	
State University of New York, Stony Brook	David Sprouster (Co-Principal Investigator)	
Brookhaven National Laboratory	Mehmet Topsakal (NSUF Technical Lead)	

SHORT COMMUNICATIONS

In situ TEM Studies on Thermodynamic Stability and Microstructural Evolution of Zirconium Hydrides in Irradiation and Thermal Environments

Caitlin Kohnert - Los Alamos National Laboratory - caitlin@lanl.gov



The goal of this research project is to investigate the radiation response of zirconium hydride at various temperatures. Brittle hydrides form in zirconium cladding and are the primary degradation mechanism. Understanding how these hydrides react with temperature and radiation is of utmost importance for understanding cladding degradation and thus learning how to extend cladding lifetimes. Phase stability was examined as a function of irradiation dose and temperature in order to elucidate irradiationinduced changes in phase stability, which is of significant relevance to hydride-moderator performance in microreactor and space-reactor applications.

Experimental or Technical Approach

In situ transmission electron microscopy (TEM) ion irradiations were conducted at the Intermediate Voltage Electron Microscope (IVEM) Facility at Argonne National Laboratory. TEM lamellae were precharacterized using a combination of bright-field and dark-field imaging, along with selected-area diffraction. Regions with multiple grains were chosen to aid in the identification of new phases. Under- and overfocus conditions were explored to check for preexisting voids. The sample was then heated to the testing temperature; subsequently, another round of characterization was conducted. The sample was then exposed to a 1 MeV krypton-ion

beam to induce displacement damage without implantation. Videos were taken during the heating and irradiation. Diffraction patterns were also included in the irradiation videos to determine the dose at which the phase change occurred. Following a 100 min irradiation, corresponding to 8 dpa, a post-irradiation characterization was conducted. Diffraction patterns were then analyzed using the single crystal suite of software. As multiple grains were present, and the patterns were not taken down zone, ring fitting was used to identify the phases present.

Results

Analyzing the before and after diffraction patterns revealed that, under purely thermal annealing at 540°C, the loss of hydrogen was accompanied by a phase transformation to alpha zirconium. This is contrasted by the irradiated samples at and above 200°C, which appear to have transformed into beta zirconium. A comparison of the diffraction patterns of the 400°C irradiated sample to the 600°C annealing sample is shown in Figure 1. The room temperature samples showed no signs of phase change.

To try and deconvolve the effect of temperature and irradiation, thermal-annealing experiments were conducted at 400°C at Los Alamos National Laboratory. The sample was prepared from the same bulk pieces from which the original IVEM foils were made using the same microscopes. In situ TEM annealing was then conducted using a Thermo Fisher Titan TEM. The temperature steps and durations were copied from the logs taken at IVEM. It was found that pure thermal annealing at 400°C resulted in a phase transformation into alpha zirconium, as happened in the the 600°C experiment, but without sudden dehydriding. A 200°C experiment is planned, but has not been completed at this time.

Discussion/Conclusion

It was found that, above 200°C, delta zirconium hydride is not stable under irradiation; instead, it transforms into the beta zirconium phase. However, under purely thermal regimes at above 400°C, delta zirconium hydride dehydrides into the thermodynamically predicted alpha-zirconium phase. This finding suggests that irradiation stabilizes the beta-zirconium phase, which could create a lattice mismatch in the cladding material. Further studies on more bulk-scale material should be conducted to remove any possibilities of this being a thin-film effect.

Distributed Partnership at a Glance		
NSUF Institution	Facilities and Capabilities	
Argonne National Laboratory	The Intermediate Voltage Electron Microscopy (IVEM) — Tandem Facility	
Collaborators		
Montanuniversitat Leoben, Austria	Matheus Tunes (Co-Principal Investigator)	
University of California, Berkeley and Los Alamos	Darren Parkison (Co-Principal Investigator)	
Los Alamos National Laboratory	Tarik Saleh (Team Member) Aditya Shivprasad (Team Member)	

Irradiation Behavior of Nanostructured Ferritic/Martensitic Grade 91 Steel at High Dose

Dr. Haiming Wen - Missouri University of Science and Technology - wenha@mst.edu



anostructured steels have been indicated to possess significantly improved mechanical properties and enhanced irradiation tolerance over conventional steels [1-5]. However, radiation-damage studies of these materials are very limited, and radiation effects—especially radiation-induced segregation and precipitation—as a function of grain size and irradiation temperature remain largely unknown. This project sought to establish the radiation effects in these materials under ion irradiation at different temperatures to high dose. The research team hypothesized that the radiation-induced segregation and precipitation in nanostructured alloys would be notably reduced as compared to those in conventional coarse-grained (CG) counterparts.

Experimental or Technical Approach

Samples of equal and uniform thickness (~1 mm) were cut from bulk stock of as-received CG, ultrafine grained (UFG) ferritic/ martensitic Grade 91 steel achieved through equal-channel angular

pressing (ECAP), and nanocrystalline (NC) achieved through highpressure torsion (HPT). The CG grain diameter was $>1 \mu m$, UFG was 100 nm < grain diameter < 1 µm and NC grain diameter was <100 nm. The samples were then mechanically polished with a final step of 0.02 um colloidal silica. The polished samples were then sent to the University of Michigan Ion Beam Laboratory for ion irradiation at multiple temperatures. CG, UFG, and NC Grade 91 samples were irradiated with Fe2+ ions to a target of 200 dpa at a depth of ~600 nm at room temperature, and at 300°C, 400°C, 450°C, and 500°C. After irradiation, the room-temperature and 450°C irradiated samples were sent to the Center for Advanced Energy Studies for characterization. Characterization included nanoindentation followed by transmission electron microscopy (TEM) sample preparation through focused ion beam techniques in a dual-beam scanning electron microscope. Detailed TEM characterization was also performed using a probe-corrected Thermo Fisher Scientific Spectra microscope. Such characterization included

scanning transmission electron microscopy (STEM), bright-field and high-angle annular dark field imaging, as well as energy dispersive x-ray spectroscopy (EDS). Detailed microstructural TEM characterization of the irradiated regions were then performed to determine the effects of radiation on microstructure, focusing on radiation-induced defect formation, solute segregation, and precipitation.

Results

Nanoindentation was performed at multiple indentation depths to provide initial mechanical comparison. Unfortunately, due to poor surface conditions after irradiation, hardness values for the 450°C irradiated samples were considered invalid. Nonetheless, in comparing unirradiated samples and room-temperature irradiated samples, differences in hardness were observed. More specifically, effects of grain size for CG, at an indent depth of 200 nm, were seen in terms of a hardness increase of hardness of 1.39 GPa; for the UFG, the increase was 1.26 GPa, and for NC, a hardness decrease of 0.23 GPa was observed. Using STEM

images, it was observed that void formation is not prevalent in the irradiated samples, even in the CG condition, but significant void formation is observed in the 450°C irradiated samples. EDS provides compositional data for identification of precipitates and segregation, and it was observed that significant segregation occurred around believed dislocation loops in the NC Grade 91 when irradiated at 450°C.

Discussion/Conclusion

Void density with grain size decrease in the 450°C irradiated samples. This indicates that grain boundaries are acting as effective sinks for vacancies. However, in the NC sample irradiated at 450°C, a significant network of believed dislocation loops were formed, and such features are not observed in the other conditions. An apparent denuded zone around a grain boundary was observed in the NC 450°C sample, still indicating an effective sink. The minimal change in hardness between the unirradiated NC condition and the RT irradiated NC condition indicates that irradiation resistance was improved.

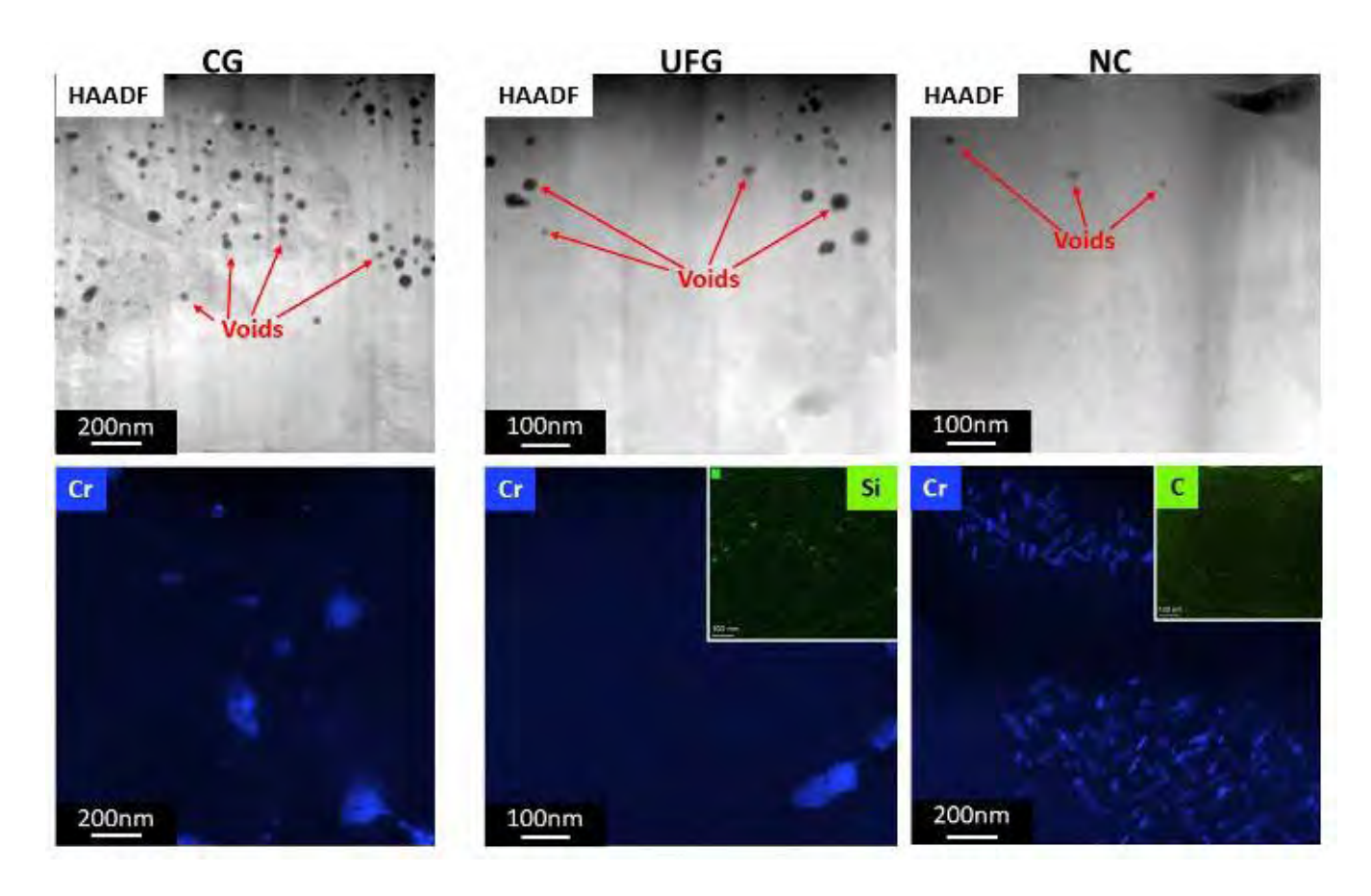


Figure 1. High-angle annular dark-field scanning transmission electron microscopy (STEM) images and corresponding select energy-dispersive x-ray spectroscopy maps of CG, UFG, and NC Grade 91 ion irradiated to 200 dpa at 450° C.

References

- [1.] C. Sun, K.Y. Yu, J.H. Lee, Y. Liu, H. Wang, L. Shao, S.A. Maloy, K.T. Hartwig, X. Zhang, Enhanced radiation tolerance of ultrafine grained Fe–Cr–Ni alloy, Journal of Nuclear Materials 420 (2012) 235–240. https://doi.org/10.1016/J. JNUCMAT.2011.10.001.
- [2.] A. Alsabbagh, A. Sarkar, B. Miller, J. Burns, L. Squires, D. Porter, J.I. Cole, K.L. Murty, Microstructure and mechanical behavior of neutron irradiated ultrafine grained ferritic steel, Materials Science and Engineering: A 615 (2014) 128–138. https://doi.org/10.1016/J. MSEA.2014.07.070.
- [3.] M. Song, Y.D. Wu, D. Chen, X.M. Wang, C. Sun, K.Y. Yu, Y. Chen, L. Shao, Y. Yang, K.T. Hartwig, X. Zhang, Response of equal channel angular extrusion processed ultrafine-grained T91 steel subjected to high temperature heavy ion irradiation, Acta Mater 74 (2014) 285–295. https://doi.org/10.1016/J. ACTAMAT.2014.04.034.

- [4.] C. Sun, S. Zheng, C.C. Wei, Y. Wu, L. Shao, Y. Yang, K.T. Hartwig, S.A. Maloy, S.J. Zinkle, T.R. Allen, H. Wang, X. Zhang, Superior radiation-resistant nanoengineered austenitic 304L stainless steel for applications in extreme radiation environments, Scientific Reports 2015 5:1 5 (2015) 1–7. https://doi.org/10.1038/srep07801.
- [5.] J. Duan, H. Wen, L. He, K. Sridharan, A. Hoffman, M. Arivu, X. He, R. Islamgaliev, R. Valiev, Effect of grain size on the irradiation response of grade 91 steel subjected to Fe ion irradiation at 300°C, J Mater Sci 57 (2022) 13767–13778. https://doi.org/10.1007/s10853-022-07480-6.

Distributed Partnership at a Glance				
NSUF Institution	Facilities and Capabilities			
Center for Advanced Energy Studies	Microscopy and Characterization Suite (MaCS)			
University of Michigan:	Michigan Ion Beam Laboratory			
Collaborators				
Missouri University of Science and Technology	Joshua Rittenhouse (Co-Principal Investigator)			
Center for Advanced Energy Studies	Yu Lu (Team Member) Jana Howard (Team Member)			
University of Michigan Ion Beam Laboratory	Zhijie (George) Jiao (Team Member)			

Micromechanical Testing of LWR-Irradiated Harvested Reactor Internals

Jason Daniel - Nucleur Regulatory Commission - Jason. Daniel@nrc.gov



enerally, irradiation-assisted stress corrosion cracking growth-rate tests on Zorita materials below 20 dpa have not shown a tendency for high cracking growth rates (CGR's), while tests at levels above 20 dpa have shown greater potential for a high CGR. Tensile testing showed a change in failure mode from ductile failure at lower doses (10 and 25 dpa) to intergranular failure at the highest dose (50 dpa). The goal of this project was to investigate, as a function of dose (<1, 15, and 50 dpa), the changes in grain-boundary (GB) behavior, including potential GB weakening, of the Zorita materials with increasing fluence.

Experimental or Technical Approach

Stainless steel (SS) 304 rector components internals irradiated in a light-water reactor were harvested and used for this study. Three 3 mm disks were used for mechanical characterization. The 0.05-dpa 3-mm disk was electropolished too thin; thus, it was deemed compromised and would not be representative of components at this dose. Due to the limited total volume available of the intact 15 dpa and 50 dpa samples, two adjacent grains containing a randomly oriented high-angle GB between them were selected as specimen sites. These locations were chosen to minimize sampleto-sample variability and promote GB failure, if it were to occur, to estimate GB strength. Bi-crystalline microtensile specimens were fabricated using the ThermoFisher Helios G4 DualBeam xenon-plasma focused-ion beam. The 50 dpa disk contained two specimens tested at room temperature (RT) and four tested at 300°C. The 15 dpa disk contained two specimens tested at RT and three at 300°C. Test videos of each specimen, along with the load-displacement readouts from the load cell, were recorded.

Results

The table below presents the mechanical property data determined for each microtensile specimen pulled, along with the averaged data for each mechanical property measured at RT and 300°C for the 15-dpa and 50-dpa specimens. Test Specimen 3 in the 15-dpa disk pulled at RT was unloaded after observable plastic deformation and then reloaded to failure. The digital image-correlation tracking software was unable to track, accurately and sufficiently, the linear elastic region of 50-dpa Specimen 4, pulled at RT, to produce a representative elastic modulus; thus, this value is omitted. None of the bi-crystalline microtensile specimens failed along their GBs; instead, they underwent significant deformation-slip behavior. In a

Irradiation Condition	Test Temperature [°C]	Test Number		σ _{γταν} [MPa]	ε _{max-raw} [%]	E [GPa]	σ _{γ-οις} [MPa] 709	ε _{max-DIC} [%]	σ _{max} [MPa]
15 dpa	RT			710					
		3	Test 1	871	56.0	187	872	10.9*	946
			Test 2	925	58.1	198	901	32.1	935
		Average		835 ± 112	56.9 ± 1.1	197 ± 10	827 ± 104	30.1 ± 2.9	873 ± 118
	300 °C	2		688	54.3	160	609	36.8	712
		4		679	53.1	133	538	50.2	700
		5		645	61.0	156	641	41.6	707
		Av	erage	671 ± 23	56.1 ± 4.3	150 ± 15	596 ± 53	42.9 ± 6.8	706 ± 6
50 dpa	RT		3	672	87.0	170	660	27.3	672
		4		537	66.7		420	55.0	591
		Av	erage	605 ± 95	76.9 ± 14.4	170	540 ± 170	41.2 ± 19.6	632 ± 57
	300 °C		1	356	33.2	109	382	19.7	404
			6	641	50.2	189	647	30.0	694
		7		502	50.4	166	486	44.7	508
			9	528	35.4	112	483	29.8	572
		Av	erage	507 ± 117	42.3 ± 9.3	144 ± 40	500 ± 110	31.1 ± 10.3	545 ± 121

^{*}Unloaded well before failure.

few cases when testing at 300°C, necking-type behavior of the gages occurred prior to ultimate failure: 15-dpa Specimens 2 and 4 and 50dpa Specimen 1, where the gage is heavily elongated and there is a drastic reduction in cross-sectional area prior to ultimate failure. All other specimens exhibited more rigid deck-of-cards-like deformationslip behavior along one or more slip planes until one slid to the point where the gage completely separated, ending in ultimate failure. These specimens fractured without portions of their gages having greatly reduced cross-sectional areas.

Discussion/Conclusion

Microtensile testing of material at 15 and 50 dpa was employed to develop trends in the mechanical properties of the Zorita 304 SS as a function of irradiation dose and test temperature. Irradiation strengthening occurs as the dose

increases from 0 to 15 dpa. At 50 dpa, the material microstructure has more heterogeneity, and this is reflected in the broader range of yield stresses measured from mechanical testing and estimated using microstructural data.

Distributed Partnership at a Glance					
NSUF Institution	Facilities and Capabilities				
Idaho National Laboratory	Analytical Laboratory				
	Irradiated Materials Characterization Laboratory (IMCL)				
Collaborators					
Idaho National Laboratory	Mukesh Bachhav (Team Member) Sriswaroop Dasari (Team Member) Cameron Howard (Team Member) Boopathy Kombaiah (Team Member) Sohail Shah (Team Member) Fei Teng (Team Member) Yachun Wang (Team Member)				

Irradiation Effects on Microstructure and Mechanical Properties in a Laser-Welded ODS Alloy

Matthew Swenson - University of Idaho - swenson@uidaho.edu

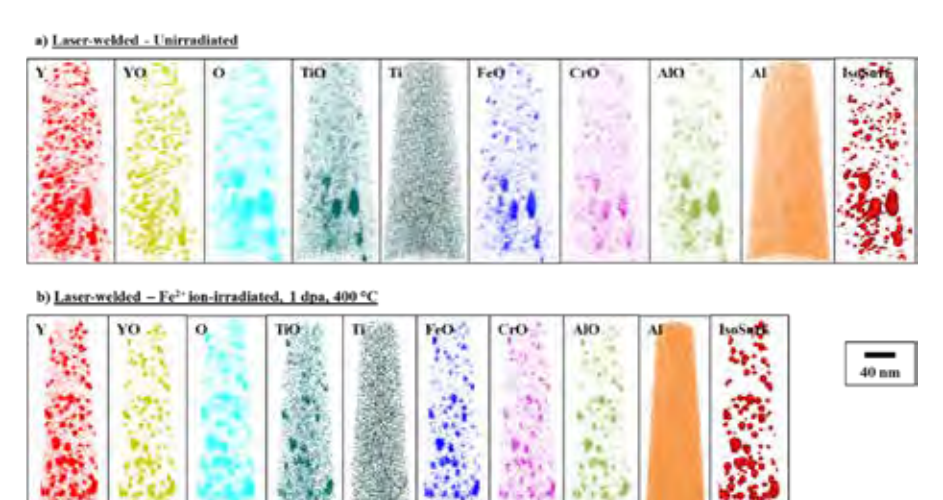


he objective of this project is to evaluate the combined effects of laser-weld joining and irradiation on the microstructure and mechanical properties of a commercial oxide-dispersionstrengthened (ODS) alloy, MA956, for advanced nuclear reactor applications. The focus of this Rapid-Turnaround Experiment (RTE) is on post-irradiation examination (PIE) and microscopy activities, which enable characterization and description of the combined effects of both laser welding and ion irradiation on the alloy's performance.

Experimental or Technical Approach

Laser welding of MA956 specimens was completed at MacKay Manufacturing, Inc., in Spokane, Washington, via welding two physical pieces together. Laserwelded samples were subsequently irradiated at Sandia National Laboratory with Fe2+ ions at 400°C to 1 dpa, and separately to 25 dpa. PIE was executed via access to the Microscopy and Characterization Suite (MaCS) at the Center for Advanced Energy Studies. A focused ion beam was used to fabricate local electrode atom probe (LEAP) and transmission electron microscopy samples. Characterization was completed via scanning transmission

Figure 1. Representative solute reconstructions of laser-welded MA956: a) unirradiated and b) irradiated with Fe2+ ions at 400°C to 1 dpa.



electron microscopy imaging with the SuperX energy-dispersive spectroscopy ChemiSTEM facilities and with the LEAP at MaCS. This experiment was also designed to enable direct comparison with prior characterization results from frictionstir welding of the same MA956 alloy (accomplished via RTE 17-906) to the same 1 dpa and 25 dpa irradiation conditions. Needles for LEAP analysis were lifted from within the laser-welded region of the joint in the unirradiated condition, and following irradiation to 1 dpa and 25 dpa, respectively. ChemiSTEM and electron backscatter diffraction (EBSD) imaging was conducted on each of the samples.

Results

The average size and number density of the oxide nanoclusters were found to be 5.44 ± 0.11 nm and 179×10^{21} m⁻³, respectively. This is a finer morphology than that found in the bulk unwelded material from a prior RTE project [1], which exhibited a size and number density of 7.42 ± 0.10 nm and 40×10^{21} m⁻³, respectively. Interestingly, after irradiation with Fe²⁺ ions to 1 dpa at 400° C, the oxide nanoclusters had coarsened, with a resulting size and number density

of 6.09 ± 0.18 nm and 115×10^{21} m⁻³, respectively. This initial result confirms that oxide nanoclusters can survive the laser-welding process, and indicates that the oxide nanoclusters may be stable upon irradiation to a low dose. EBSD imaging indicates that, in addition to the growth of columnar grains, there are large voids throughout the weld. Dispersoids are found to coarsen following laser welding.

Discussion/Conclusion

One of the project's aims is to understand how the laser-welding process will disrupt microstructure in a typical ferritic alloy with nanoscale oxide particles in the matrix. Although the first attempt at laser welding did not produce a perfect joint, it has demonstrated that using the laser-welding process makes it possible to retain the beneficial oxide nanoparticles within the material. At low dose, the oxides present within the weld appear to be reasonably stable upon

irradiation, suggesting that welding could someday be a viable option for welding ODS and other ferritic nanofeatured alloys.

References

[1.] E. Getto, M. Johnson, M.R.
Maughan, N. Nathan, J.
McMahan, B. Baker. K.
Knipling, S. Briggs, K.
Hattar, M.J. Swenson.
Friction stir welding and self-ion irradiation effects on microstructure and mechanical properties changes within Oxide
Dispersion Strengthened Steel
MA956, J. of Nucl. Mat. (2022)
153795.

Distributed Partnership at a Glance		
NSUF Institution	Facilities and Capabilities	
Center for Advanced Energy Studies	Microscopy and Characterization Suite (MaCS)	
Collaborators		
U.S. Naval Academy	Elizabeth Getto (Co-Principal Investigator) Brad Baker (Team Member)	
University of Idaho	Ryan Sundburg (Graduate Student)	

Examining Microstructures and Mechanical Properties of Neutron- and Ion-irradiated T91, HT9, and Alloy 800H

Pengcheng Zhu - The University of Tennessee, Knoxville - pzhu2@alum.utk.edu



on irradiation has been considered as a surrogate for reactor irradiations and has been widely used due to its versatility, including investigations of high damage rate and low radioactivity. A successful simulation requires similarities, not only in neutronmodified microstructures but also in neutron-induced bulk properties, to those caused by ion irradiation. In prior studies, however, accurate comparison of mechanical properties between neutron and ion irradiations are rare. Additionally, the correlation between microstructures and mechanical properties has not been rigorously evaluated. The goal of this research project is to systematically investigate the microstructural evolution and mechanical properties of neutron- and dual-ion irradiated in T91, HT9, and 800H alloys at varied temperatures and damage levels to provide more insight into the fidelity of ion-beam simulation of neutron irradiation.

Experimental or Technical Approach

Ferritic/martensitic steels T91 and HT9 and austenitic alloy 800H were irradiated with neutrons (in the BOR60 reactor) and dual ions (9 MeV Fe3+ and 3.24 MeV He2+) at 376-520°C with damage from 16.6 to 72 dpa, to quantify the possibility of using ion irradiation to simulate neutron irradiation in terms of microstructures and mechanical properties. The irradiation temperature is selected to have a temperature shift about 60°C between the neutron irradiation and ion irradiation. Nanoindentation testing was performed to obtain the bulk hardness of the dualion-irradiated samples, due to limited damage volumes. For the neutron-irradiated samples, both nanoindentation and Vickers hardness testing were conducted. An accurate method of extracting bulk hardness from nanoindentation data was used, based on our previous study on FeCr alloys.

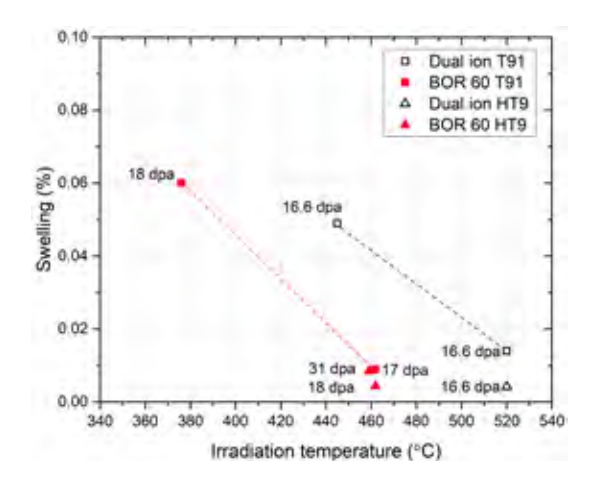


Fig. 1 Volume swelling for the dual-ion- and neutron-irradiated T91 and HT9 samples.

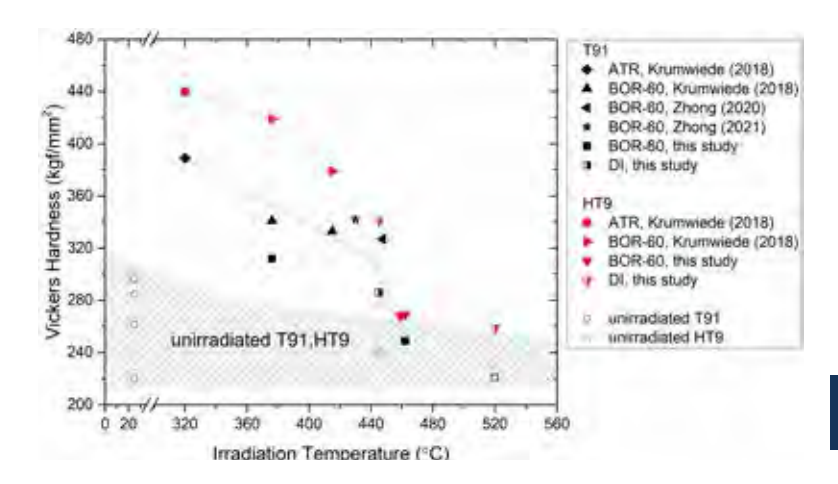


Fig. 2 Evolution of Vickers hardness with irradiation temperature (Ref. [1–4] for irradiated samples, Ref. [2,5,6] for unirradiated samples). Vickers hardness for unirradiated samples at high temperature refers to testing on unirradiated regions of dual-ion-irradiated samples (see Section 2). ATR refers to the Advanced Test Reactor at Idaho National Laboratory.

Transmission electron microscopy (TEM) characterization of the cavities, dislocation loops, and precipitates was conducted to account for the strengthening contribution of each microstructure element. Precipitates and radiation-induced segregation were characterized by energy-dispersive spectroscopy mapping and energy-dispersive spectroscopy on a Talos TEM. The over- and underfocus technique was applied to image the cavities in both neutron- and ion-irradiated samples.

Results

Shown in Fig. 1, the temperature shift of about 60°C provided a general match between neutron and ion irradiation for the peak

swelling-temperature shift, but there is a larger discrepancy between the theoretical and experimental values for the cessation of swelling. When comparing the mechanical properties of neutron- and ionirradiated samples, Fig. 2 exhibits that a pronounced irradiation hardening occurred below about 420°C, followed by a rapid decrease of hardness in the 420–460°C regime. However, in that same regime, the hardness values of ion-irradiated samples (represented by the halfopen symbols in Fig. 2) are close to the temperature-dependent trend of neutron samples. This indicates that a simple 60°C temperature shift may not be suitable for the entire broad temperature range (320-520°C). For

the correlation between the model's predicted and measured strengths (converted from nanoindentation) of the neutron- and ion-irradiated samples, the data points fall close to the ideal 1:1 line, as shown in Fig. 3. This good agreement demonstrates the feasibility of using the strengthening model, as well as the superposition method, in this study to predict strengths from the microstructure aspects.

Discussion/Conclusion

The temperature-shift theory works generally well for cavities and dislocation loops observed in T91 following ion and neutron irradiations, but it is not suitable for matching precipitates. This is especially true for the HT9 material, where both dislocation loop and precipitate evolution did not follow the calculated temperature shift.

The comparable nanoindentation results from dual-ion- and neutron-irradiated T91 and HT9 at elevated temperatures (>450°C) may largely be due to minimal irradiation hardening at elevated temperatures. The discrepancy in the microstructures indicates that morecomplex modeling should be used to link ion- vs neutron-irradiation microstructures and hardening.

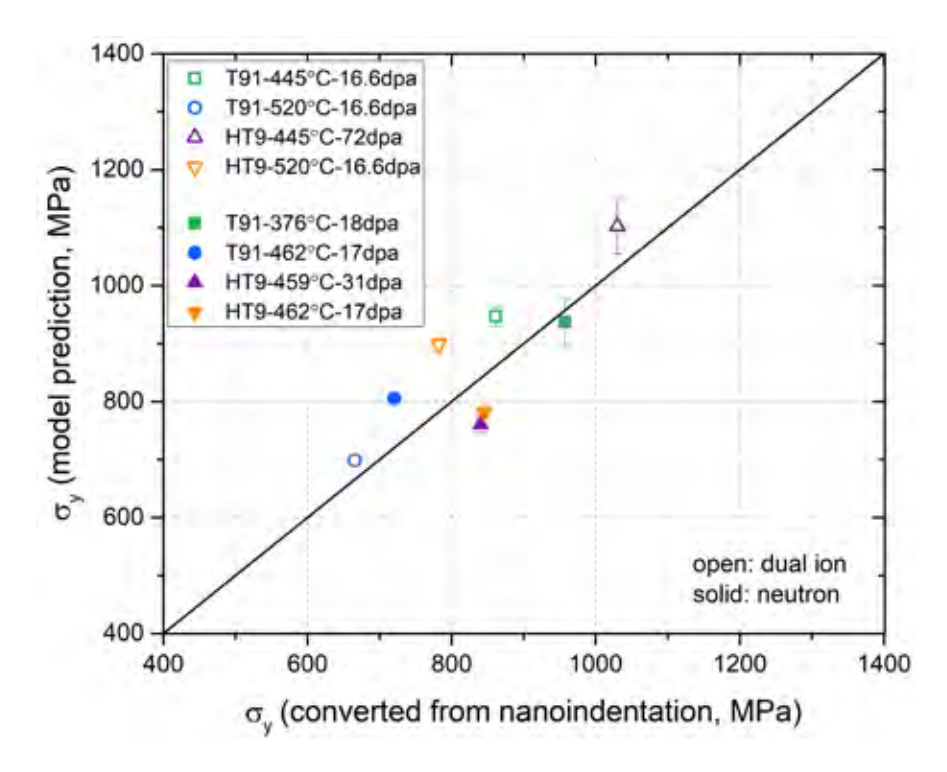


Fig. 3 Correlation between the model-predicted strength and measured strength.

References

- [1.] D.L. Krumwiede, Correlation of Nanohardness to Bulk Mechanical Tensile and Shear Properties through Direct Characterization and Comparison of Neutron-Irradiated Steels, UC Berkeley, 2018. https://escholarship.org/uc/item/1qv0h8fk.
- [2.] D.L. Krumwiede, T. Yamamoto, T.A. Saleh, S.A. Maloy, G.R. Odette, P. Hosemann, Direct comparison of nanoindentation and tensile test results on reactorirradiated materials, J. Nucl. Mater. 504 (2018) 135–143.

- [3.] W. Zhong, L. Tan, Report on partially complete post-irradiation-examination of the INL samples, 2020. https://doi.org/10.2172/1651352.
- [4.] W. Zhong, T.A. Saleh, L. Tan, Neutron irradiation induced defects and clustering in NF616 and T91, J. Nucl. Mater. 552 (2021) 153001. https://doi.org/10.1016/j. jnucmat.2021.153001.
- [5.] T.R.G. Kutty, K. Ravi, S. Kaity, S.K. Swarnkar, A. Kumar, Effect of temperature on hardness of binary U–15%Pu alloy

- and T91 cladding, J. Nucl. Mater. 429 (2012) 341–345. https://doi.org/10.1016/j. jnucmat.2012.06.025.
- [6.] A. Prasitthipayong, D. Frazer, A. Kareer, M.D. Abad, A. Garner, B. Joni, T. Ungar, G. Ribarik, M. Preuss, L. Balogh, S.J. Tumey, A.M. Minor, P. Hosemann, Micro mechanical testing of candidate structural alloys for Gen-IV nuclear reactors, Nucl. Mater. Energy. 16 (2018) 34–45. https://doi.org/10.1016/j. nme.2018.05.018.

Distributed Partnership at a Glance		
NSUF Institution	Facilities and Capabilities	
Oak Ridge National Laboratory	Low Activation Materials Design and Analysis Laboratory (LAMDA)	
Collaborators		
Oak Ridge National Laboratory	Yan-Ru Lin (Team Member)	
The University of Tennessee, Knoxville	Shradha Agarwal (Team Member) Steven Zinkle (Team Member)	

Neutron Irradiation Effects on the Tensile Properties of Wire Arc Additive Manufactured Grade 91 Steel

T.M. Kelsy Green - Oak Ridge National Laboratory - tmkgreen@lanl.gov



he ferritic-martensitic (FM) alloy Grade 91 is a candidate structural material for advanced fission reactors. To create finer microstructural features for radiation tolerance, Grade 91 was fabricated via wire-arc additive manufacturing (AM), the secondever print recorded. Though the unirradiated properties of the as-printed and heat-treated wire-arc additive-manufacturing (WAAM) Grade 91 are promising [1], an investigation of WAAM Grade 91's behavior under neutron irradiation is necessary for nuclear applications. This work conducted tensile tests on neutron-irradiated WAAM Grade 91 with the goal of capturing its low-dose mechanical response and laying the groundwork for understanding irradiated AM-FM alloy behavior.

Experimental or Technical Approach

Bulk samples of as-printed and heat-treated—to 1100°C for 30 min and 760°C for 60min—WAAM Grade 91 were machined into SS J2-type tensile specimens before being loaded in the High Flux Isotope Reactor. As-printed specimens were machined from the X (i.e., perpendicular to the build direction) and Z (i.e., parallel to build direction) orientations of the bulk sample. Samples were irradiated to approximately 0.7 and 2.1 dpa at 300 ±50°C. After irradiation, room-temperature tensile testing mediated with digital image correlation (DIC) was conducted to provide data on strain hardening in WAAM Grade 91 as a function of dose, specimen-build direction, and heat treatment [2]. Scanning electron microscopy

characterization of the post-test fracture surfaces was also conducted with the use of radiation facilities. To allow for easy determination of the radiation response, the in-facility tensile tests were conducted on a universal load frame in air under the same conditions as the unirradiated WAAM Grade 91 specimens. All the tensile tests were performed with a strain rate of 10⁻³ s⁻¹ using shoulder loading. One tensile test per condition was tested.

Results

This work is the first ever to explore the tensile properties of neutron-irradiated WAAM Grade 91, providing significant contributions to the study of AM for advanced-reactor applications. The tensile tests helped determine WAAM Grade 91's in-reactor property evolution in its as-printed and heat-treated states. First, the unirradiated tensile specimens from the as-printed X-direction displayed less strain hardening than the as-printed

Z-direction specimen. Second, heat treatment caused the unirradiated tensile specimens from the X-direction to increase in ductility, but reduced their yield and ultimate tensile strength. Correlative DIC captured this effect by displaying different strain-rate behaviors in the as-printed and heat-treated unirradiated X-cuts. DIC showed one localized region of deformation in the gauge of the as-printed X-cut, as opposed to uniform strain across the gauge in the heat-treated X-cut, up to the ultimate tensile strength followed by strain localization in the necking region. Third, irradiation to 0.7 and 2.1 dpa caused both the X- and Z-cuts to have increased yield strength and decreased ductility. This effect was most pronounced as a function of increasing dose in the Z-cut, where the unirradiated specimen displayed moderate strain hardening before failure, but almost no strain hardening after 2.1 dpa.

Wire arc AM Grade 91

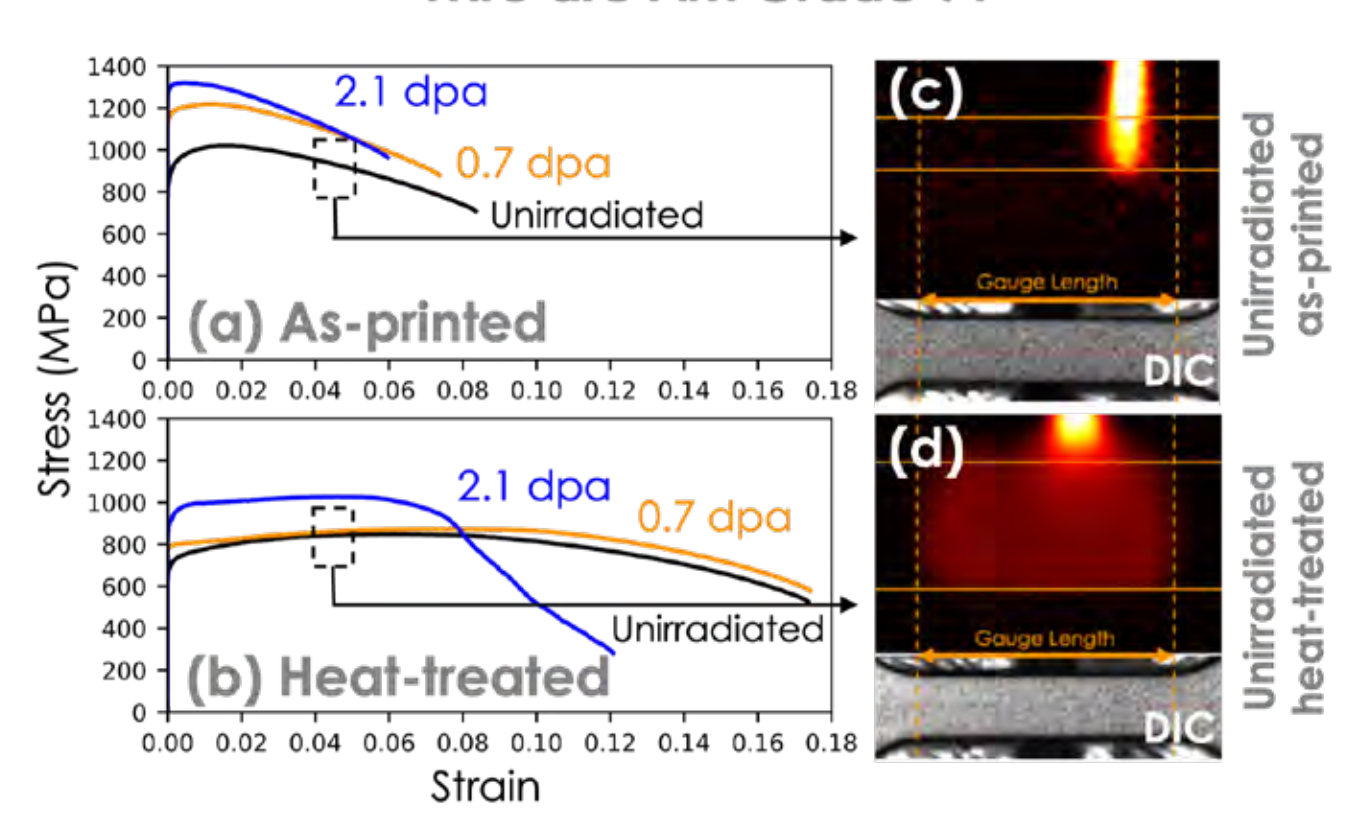


Figure 1. Stress-strain curves of tensile specimens from the X-direction for the unirradiated and irradiated conditions (neutron irradiated to 0.7 and 2.1 dpa) in the (a) as-printed condition and (b) heat-treated condition of WAAM Grade 91 steel. The corresponding strain-rate maps across the gauge lengths of the unirradiated (c) as-printed and (d) heat-treated samples are also shown (taken with DIC).

Discussion/Conclusion

The hardening behavior in WAAM Grade 91 displays anisotropic unirradiated properties, which are also anisotropic after low-dose neutron irradiation. Thus, tensile tests should be conducted on samples taken perpendicular and parallel to the build direction. Additionally, build parameters may be modified to alleviate the anisotropic behavior.

Heat treating WAAM FM steel after fabrication may lead to comparable mechanical properties in wrought FM steels. It is hypothesized that the initial high sink strength of the as-printed specimens (derived mainly from dislocations and grain structures) caused less strain hardening, which led to the faster onset of radiation-induced saturation of deformation.

References

- [1.] T.M.K. Green, N. Sridharan, X. Chen, K.G. Field, Effect of N2- and CO2-containing shielding gases on composition modification and carbonitride precipitation in wire arc additive manufactured grade 91 steel, Addit Manuf. 56 (2022). https://doi.org/10.1016/j. addma.2022.102854.
- [2.] K.G. Field, S.A. Briggs, K. Sridharan, R.H. Howard, Y. Yamamoto, Mechanical properties of neutron irradiated model and commercial FeCrAl alloys, Journal of Nuclear Materials 489 (2017) 118–128. https://doi.org/10.1016/j.jnucmat.2017.03.038.

Distributed Partnership at a Glance	
NSUF Institution	Facilities and Capabilities
Oak Ridge National Laboratory	High Flux Isotope Reactor (HFIR) Irradiated Materials Examination and Testing Facility (IMET) Hot Cells Low Activation Materials Design and Analysis Laboratory (LAMDA)
Collaborators	
Oak Ridge National Laboratory	Caleb Massey (Team Member)
University of Michigan-Ann Arbor	Kevin G. Field (Team Member)

Hydrogen-Retention of Yttrium Hydride Under High-Temperature Proton Irradiation

Timothy G. Lach - Oak Ridge National Laboratory - lachtg@ornl.gov



his project aimed to investigate the phase stability and hydrogen retention of yttrium hydride under high-temperature proton irradiation. The research team hypothesized that radiation would reduce the onset temperature for hydrogen desorption and that lower energy recoils would generate increasing hydrogen release with irradiation temperature, due to preferential displacement of H over Y from the lattice due to their difference in mass. The outcome of this work will provide quantitative comparisons of hydrogen desorption and hydride phase stability as a function of irradiation temperature and recoil energy. This knowledge is critical to understanding how hydrogen transport in metal hydrides is affected by irradiation and how to mitigate radiationinduced degradation in solid moderator materials.

Experimental or Technical Approach

Yttrium hydride, fabricated as part of the Transformational Challenge Reactor Program [1-3], was irradiated with high-energy proton irradiation and characterized using elastic-recoil detection analysis (ERDA), electron microscopy, and Raman spectroscopy. Ion irradiations were performed with either 1 MeV H+ ions or 2 MeV H+ ions, using the 3 MV Pelletron accelerator at the Michigan Ion Beam Laboratory (MIBL) at two temperatures relevant to advancedreactor environments. ERDA is a highly sensitive surface ionbeam analysis technique capable of detecting depth-dependent hydrogen concentrations down to 0.1 at%. Before each ion irradiation, the hydrogen concentration was measured using ERDA on multiple surface spots at MIBL, and again after ion irradiation in both the irradiated and non-irradiated

portions to separate the effects of high temperatures and radiation damage. Additional characterization was performed using transmission electron microscopy and Raman spectroscopy at the Low Activation Materials Development and Analysis Facility to understand the radiation-damage mechanisms and microstructural evolution (dislocation loops, cavities, or other defects) and determine the pathways for hydrogen release from the ion-bombarded specimens.

Results

The results, summarized in the figure below, showed that irradiation at both proton energies and both irradiation temperatures did show hydrogen release; however, the higher-energy proton beam and higher radiation temperature resulted in greater hydrogen release. Nanocavities formed in the lower proton-energy and lower-temperature irradiation, while small dislocation loops were observed in the high proton-energy, lower-temperature regime and in the low

proton-energy, high-temperature regime. Larger dislocation loops formed after higher proton-energy and higher-temperature irradiation. These structural results correlated with the amount of hydrogen loss as measured by ERDA and backed by Raman spectroscopy results showing a greater reduction in the YH2 signal for the 2 MeV, 580°C sample than for the 1 MeV, 300°C sample. The formation of nanocavities in low proton energy and low temperatures is consistent with nanocavity formation in neutron-irradiated yttrium hydride [4], suggesting that lower-energy proton beams may better reflect mixed-spectrum fission neutron-irradiation behavior than higher-energy proton beams. The results suggest that higher irradiation temperatures and higherenergy incident beams produce a greater loss of hydrogen due to a higher density of defects formed on the Y lattice in YH2.

Discussion/Conclusion

This work revealed that the hydrogen-retention capability is proportional to the formation of traps for hydrogen atoms, and identified relative contributions of bulk- or fast-diffusion paths for hydrogen release, based on qualitative observations of the microstructure. The primary mechanisms of hydrogen loss are likely based on diffusion, but this study did not provide enough information to conclusively determine which process or combination of processes is responsible. Based on the findings, for systems using YHx as a moderator to be successful, they will likely need a hydrogen-diffusion barrier or a means to reduce the chemical potential for diffusion.

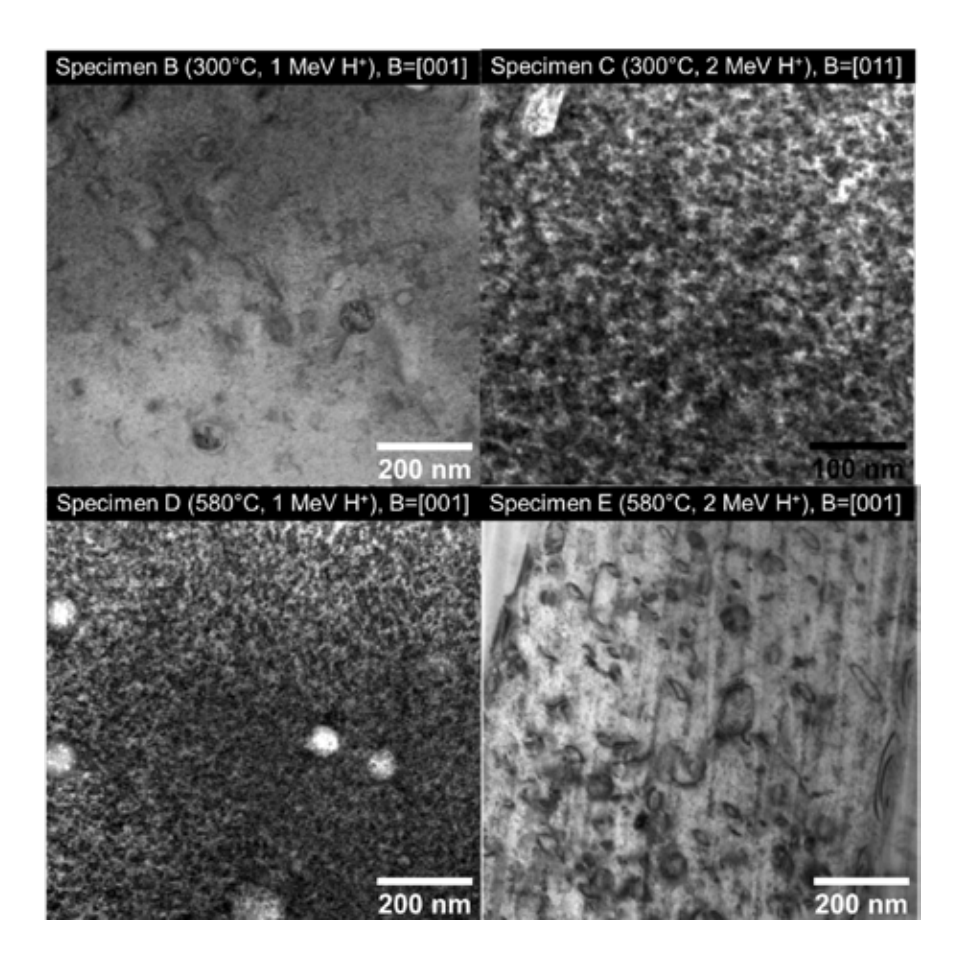


Figure 1. Scanning transmission electron microscopy bright-field images showing the dislocation microstructure for each irradiation condition. As measured per ERDA, Specimen B lost \sim 4% H, specimen C lost \sim 5% H, specimen D lost \sim 5% H, and specimen E lost \sim 11% H.

References

- [1.] X. Hu, K.A. Terrani,

 "Thermomechanical properties and microstructures of yttrium hydride, J. Alloys
 Compd. 867 (2021) 158992.

 https://doi.org/10.1016/j.
 jallcom.2021.158992.
- [2.] A.A. Trofimov, X. Hu, H. Wang, Y. Yang, K.A. Terrani, Thermophysical properties and reversible phase transitions in yttrium hydride, J. Nucl. Mater. 542 (2020) 152569. https://doi.org/10.1016/j.jnucmat.2020.152569.
- [3.] X. Hu, D. Schappel, C.M. Silva, K.A. Terrani, Fabrication of yttrium hydride for high-temperature moderator application, J. Nucl. Mater. 539 (2020) 152335. https://doi.org/10.1016/j.jnucmat.2020.152335.
- [4.] M.N. Cinbiz, T.G. Lach, M.
 Topsakal, A. LeCoq, and
 K.D. Linton. Impact of
 nano-scale cavities on
 hydrogen storage and
 retention in yttrium hydride,
 Materialia 32 (2023) 101933.
 https://doi.org/10.1016/j.
 mtla.2023.101933.

Publications

[1.] Taller, S. A., F. Naab, T. Koyanagi, and T. G. Lach, "Hydrogen-Retention Capability in the Microstructure of Yttrium Hydride under Proton Irradiation" – in preparation.

Distributed Partnership at a Glance		
NSUF Institution	Facilities and Capabilities	
Oak Ridge National Laboratory	Low Activation Materials Design and Analysis Laboratory (LAMDA)	
Collaborators		
Oak Ridge National Laboratory	Stephen A. Taller (Co-Principal Investigator) Takaaki Koyanagi (Co-Principal Investigator)	
University of Michigan	Fabian Naab (Team Member)	

NSUF LIST OF ACRONYMS

3D	three-dimensional
AI	artificial intelligence
AM	additive manufacturing
AMLActiva	ted Materials Laboratory
APS	Advanced Photon Source
ATF	accident tolerant fuel
APT	atom probe tomography
ATR	Advanced Test Reactor
BCC	body-centered cubic
BPVCboiler	and pressure vessel code
CAESCenter for A	Advanced Energy Studies
CG	coarse-grained
CGR	cracking growth rate
CINRConsolidated Inno	ovative Nuclear Research
СТ	compact-tension
DIC	digital image correlation
DOE-NE Department of Energy,	Office of Nuclear Energy
DOI	digital object identifiers
dpa	displacements per atom
EBSD electro	n backscatter diffraction
ECAPequal-c	hannel angular pressing
EELSelectron e	energy-loss spectroscopy
EDSenergy dispe	ersive x-ray spectroscopy

EFTEMenergy filtered TEM
EML Electron Microscopy Laboratory
ERDAelastic-recoil detection analysis
FMferritic-martensitic
GB grain-boundary
HAADFhigh-angle annular dark field
HFEFHot Fuel Examination Facility
HFIR High Flux Isotope Reactor
HPChigh performance computing
HPThigh pressure torsion
IMCLIrradiated Materials Characterization Laboratory
IMETIrradiated Materials Examination and Testing Facility
INLIdaho National Laboratory
INSETIn-Pile Steady State Extreme Temperature
IVEMIntermediate Voltage Electron Microscopy
LAMDALow Activation Materials Design and Analysis Laboratory
LEAPLocal Electrode Atom Probe
LWRlight water reactor
MACS Microscopy and Characterization Suite
MNSP
NCnanocrystalline
NETLNuclear Engineering Teaching Laboratory

NFMLNuclear Fuels and Materials Library ODS......oxide-dispersion strengthened OSURROhio State University Research Reactor PGAA Prompt Gamma Ray Activation Analysis PIprincipal investigator PIEpost irradiation examination PM-HIP powder metallurgy with hot isostatic pressing R&Dresearch and development RPV reactor pressure vessel RTroom temperature RTE......Rapid Turnaround Experiment SEM.....scanning electron microscope SFT.....stacking-fault tetrahedra SMRsmall modular reactor SS......stainless steel STEM.....scanning transmission electron microscope TE......total elongation TEM.....transmission electron microscope UEuniform elongation UFG......ultrafine-grained UTSultimate tensile strength VCvanadiaum carbide VN......vanadium nitride WAAMwire-arc additive-manufacturing XRD-CT.....x-ray diffraction computed tomography



INDEX

Partner Institutions

Argonne National Laboratory (ANL): 14, 18, 28, 29, 36, 38, 39, 40, 42, 43, 64, 65

Argonne National Laboratory: Advanced Photon Source (APS), 18, 86

Argonne National Laboratory: Activated Materials Laboratory (AML), 18, 28, 29, 39, 86

Argonne National Laboratory: The Intermediate Voltage Electron Microscopy (IVEM) – Tandem Facility, 14, 36, 38, 39, 40, 42, 43, 65

Belgian Center for Nuclear Research (SCK/CEN):

Belgian Reactor 2, Laboratory for High and Medium Activity, 15

Brookhaven National Laboratory (BNL): 14, 40, 61, 63

Brookhaven National Laboratory: National Synchrotron Light Source II (NSLS-II), 14, 40, 60, 63 Center for Advanced Energy Studies (CAES): 49

Idaho National Laboratory (INL): 8, 13, 22, 24, 25, 30, 32, 36, 37, 38, 39, 40, 41, 42, 43, 48, 49, 59, 71, 75, 86, 90

Idaho National Laboratory: Advanced Test Reactor (ATR), 8, 40, 43, 46, 48, 59, 75

Idaho National Laboratory: High-Performance Computing (HPC), 22, 86

Idaho National Laboratory: Irradiated Materials Characterization Laboratory (IMCL), 24, 25, 36, 37, 38, 40, 41, 42, 43, 71, 88

Idaho National Laboratory: *Materials & Fuels Complex (MFC)*, 24, 25

Lawrence Livermore National Laboratory (LLNL): 14, 38

Los Alamos National Laboratory

(LANL): 13, 14, 36, 38, 39, 42, 64, 65

Massachusetts Institute of Technology (MIT): 14, 37, 40

North Carolina State University (NCSU): 2, 13, 14, 36, 39, 40

Oak Ridge National Laboratory (ORNL): 2, 13, 14, 34, 36, 37, 38, 39, 40, 41, 60, 63, 77, 78, 81, 82, 90

Oak Ridge National Laboratory: *High Flux Isotope Reactor (HFIR)*, 2, 14, 34, 78, 81

Oak Ridge National Laboratory: Irradiated Materials Examination and Testing Facility (IMET) Hot Cells, 14, 39, 41, 81, 85, 86

Oak Ridge National Laboratory: Low Activation Materials Design and Analysis Laboratory (LAMDA), 14, 34, 36, 37, 38, 39, 40, 61, 63, 77, 81, 85,

The Ohio State University (OSU): 14, 19, 36, 37, 39, 41, 42, 43, 89, 90



The Ohio State University: *The Ohio* State University Nuclear Research Laboratory, 19

Pacific Northwest National Laboratory (PNNL): 13, 14, 40, 43

Pacific Northwest National Laboratory: *Materials Science & Technology Laboratory (MSTL)*,

Pacific Northwest National Laboratory: *Radiochemical Processing Laboratory (RPL)*, 14, 43

Penn State University: 13, 15, 39, 40

Purdue University: 13, 15, 34, 59

Sandia National Laboratories (SNL): 13, 15, 36, 39

Texas A&M University (TAMU): 15

Texas A&M University: Accelerator Laboratory, 15, 36, 37, 41, 43, 90

University of California, Berkeley (UCB): 65

University of Florida (UF): 13, 15, 36, 38, 41, 43, 90

University of Michigan (UM): 13, 15, 19, 34, 36, 39, 66, 69, 81, 85

University of Michigan: *Michigan Ion Beam Laboratory (MIBL)*, 15, 39, 41, 42, 43, 66, 69, 82

University of Michigan: Michigan Center for Materials Characterization, 15, 40

University of Wisconsin, Madison: 12, 90

University of Wisconsin: 13, 15, 43, 90

University of Wisconsin: Characterization Laboratory for Irradiated Materials, 15

Westinghouse: 14, 73

Westinghouse: *Churchill Laboratory Services*, 15, 34

Collaborators

Bachhav, Mukesh Idaho National Laboratory 71, 90

Baldo, Peter Argonne National Laboratory 90

Brillson, Leonard The Ohio State University 90

Chen, Wei-Ying Argonne National Laboratory 90

Couet, Adrien University of Wisconsin-Madison 90

Deck, Christian General Atomics 90

Di Fonzo, Fabio Italian Institute of Technology 90

Fu, Zhenyu University of Florida 89

Garner, Frank Texas A&M University 90

Gonderman, Sean General Atomics 90

He, Lingfeng Idaho National Laboratory 40, 90

Ickes, Michael Westinghouse Electric Company 90

Jiang, Wen Idaho National Laboratory 59, 90

Kombaiah, Boopathy Idaho National Laboratory 39, 71, 90

Koyanagi, Takaaki Oak Ridge National Laboratory 60, 63, 85, 90

Loiacono, Davide Italian Institute of Technology 90

Moorehead, Michael Idaho National Laboratory 37, 90

Paladino, Boris Italian Institute of Technology 90

Parkin, Calvin University of Wisconsin-Madison 39, 90

Pellemoine, Frederique Fermi National Accelerator Laboratory 90

Petrie, Christian Oak Ridge National Laboratory 90

Porter, Douglas Idaho National Laboratory 90

Shatoff, Herb General Atomics 90

Sun, Cheng Idaho National Laboratory 90

van Rooyen, Isabella Idaho National Laboratory 90

Yang, Yong University of Florida 90

Zhang, Hongliang University of Wisconsin-Madison 90



